NTIA-Report-80-54

Measurements of Electromagnetic Noise Radiated from Automotive Ignition Systems

R.J. Matheson

U.S. DEPARTMENT OF COMMERCE
Philip M. Klutznick, Secretary

Henry Geller, Assistant Secretary
for Communications and Information

November 1980

TABLE OF CONTENTS

LIST OF FIGURES

Measurements of Electromagnetic Noise Radiated From Automotive Ignition Systems

Robert J. Matheson*

Measurements of the amplitude probability distributions and the average crossing rates of the electromagnetic noise radiated by automotive ignition systems were made at 30 MHz, 47 MHz, 147 MHz, 224 MHz, and 445 MHz. The ignition noise from a single car and a 12-car matrix were each measured in a 10 kHz bandwidth, using a field-intensity meter, a DM-4, a desktop calculator, and an X-Y plotter. The DM-4 is an instrument built by NTIA to measure amplitude probability distributions and average crossing rates. Numerical integration of the amplitude probability distributions was used to determine the rms, the average, and the average logarithm of the envelope of the measured noise.

Key words: amplitude probability distributions; automotive ignition noise; electromagnetic noise; noise measurement

1. INTRODUCTION

Electromagnetic (EM) noise from automotive ignition systems can represent a major limitation to the operation of on-board radio receivers. Measurements of such radiated EM noise are not necessarily straight-forward, particularly because of the difficulties in determining what characteristics of the EM noise should be measured that will easily be related to the amount of interference caused by the noise. Traditionally, EM noise has been measured using various weighted detector functions like peak, quasipeak, rms, average voltage--all of which give a partial indication of noise characteristics. The EM noise measurements reported in this document are described in terms of amplitude probability distributions (APD) and average crossing rates (ACR), giving a greatly-improved understanding of the noise characteristics (Spaulding, 1976). The APD describes what percentage of the time the EM noise exceeds various levels; the ACR describes at what average rate the noise crosses various levels. These measurements were made using an NTIA-developed distribution meter, called the DM-4, which makes APD or ACR measurements at 31 levels spaced about 3 dB apart.

This set of measurements was made at the request of the Motor Vehicle Manufacturers Association (MVMA) to augment a set of EM noise measurements made earlier by Hartman (1980). The present set of measurements was made at the GM

*The author is with the Institute for Telecommunication Sciences, National Telecommunications and Information Administration, U.S. Department of Commerce, Boulder, CO 80302.

Proving Grounds at Milford, Michigan, during the week of April 20, 1980. In addition to the DM-4 measurement of EM noise APD's and ACR's, simultaneous measurements were made with rms and average voltage detectors. The latter set of measurements is reported elsewhere.**

2. TEST PROCEDURES

Electromagnetic noise measurements were made for two sets of cars. The first set, called the "12-car matrix," consisted of four rows of cars, each row containing three cars abreast. This configuration of cars was made up of representative samples from 5 U.S. car manufacturers and was intended to simulate the effect of 12 cars spaced closely together waiting for a traffic light to change. The second set consisted of a single car whose noise-suppressing components had been removed. This so-called "super-noisy vehicle" (SNV) was intended to provide a baseline estimate of the noise produced by a completely unsuppressed vehicle. Figure 1 shows the physical configuration of these tests. Complete sets of measurements were made at 30.2 MHz, 47 MHz, 147 MHz, 224 MHz, and 445 MHz, using horizontally and vertically polarized receiving antennas. All measurements were begun after the cars had been running a while and were idling at a normal rate. All frequencies and configurations were measured in an APD mode; some configurations and frequencies were also measured with the ACR mode. An equipment failure part way through the measurements caused the ACR measurements to give incorrect data, so ACR measurements were not made for some configurations.

The following types of APD measurements were made at all frequencies, using horizontally and vertically polarized antennas:

1. Twelve car matrix. Twelve cars and the measurement antenna arranged as shown in Figure 1. Twelve cars idling normally, SNV turned off.
2. Super-noisy vehicle (SNV). SNV and measurement antenna arranged as shown in Figure 1. SNV idling normally, twelve cars turned off.
3. Background. All cars turned off, but left in position. Measurement made on residual background noise, so that contribution of EM noise from cars can be separated from normal background EM noise. Antenna left in same position as for measurements 1 & 2.
4. System Noise. Antenna disconnected, preamplifier terminated. Shows the noise produced by the measurement system.

**Ribbens, W., University of Michigan report under MVMA Project #1110. (To be published)

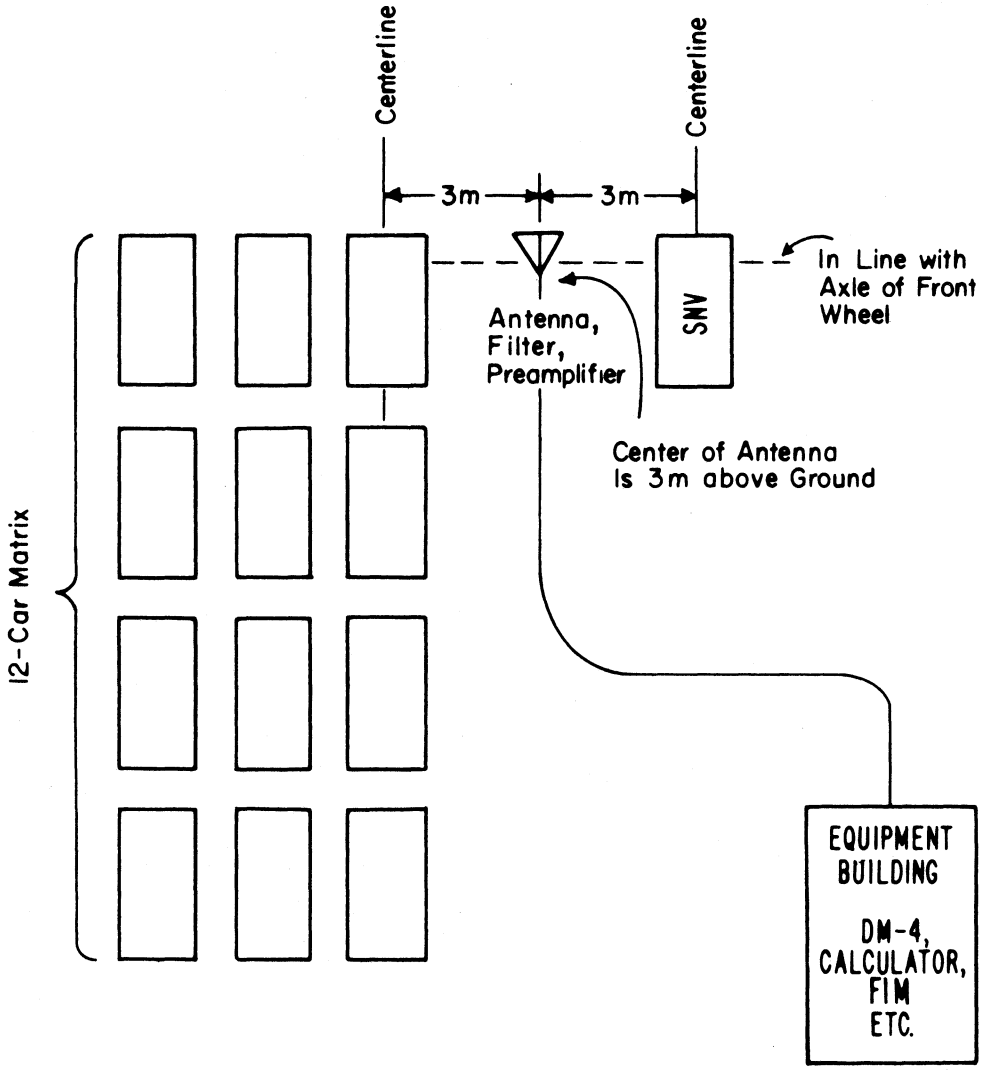

Figure 1 - Test Configuration

5. Noise Diode. Noise diode turned on and connected in place of antenna, giving 22 dB excess noise. This measurement gives a check on the proper operation of the whole measurement system. The integrated rms noise power from this calibration furnished the fundamental amplitude calibration for these measurements.

These measurements were made in a succession of configurations which allowed a minimum number of configuration changes, taking care especially to minimize the number of times that the cars had to be turned off and started. This order of measurement was generally different than the order in which the data is presented in this report.

3. INSTRUMENTATION

The measurement instrumentation is shown in Figure 2. The same equipment configuration was used at all frequencies, although different model numbers of some of the equipment was used for different frequency ranges. Table 1 shows the specific commercial types of equipment used in these measurements.

The test antenna and associated matching network are antennas designed to be used with a field intensity meter (FIM). One antenna was used for the lower 3 frequencies; another was used for the upper 2 frequencies. Both antennas are typical FIM dipole antennas with adjustable length arms, which were adjusted to manufacturers recommendations at each measurement frequency.

A tunable bandpass filter was used to isolate each measurement signal from strong signals outside each band of interest. Typically, the bandpass filter was a 5-section tunable filter with a bandpass equal to about 2% of the center frequency and an insertion loss of 2-3 dB. A wide-dynamic-range preamplifier with about 20 dB of gain was used to improve system sensitivity, especially at the higher frequencies where the transmission line to the receiver had losses of 7-8 dB. This arrangement gave system noise figures of 4-6 dB, referred to the output of the antenna matching network.

A FIM with a logarithmic video output was used as the basic receiver during these measurements, using a 10 kHz IF bandwidth. The FIM incorporated varactor-tuned tracking preselection and seemed to have adequate dynamic range for these measurements. Two signal outputs from the FIM were utilized in these measurements--the 20.4 MHz IF and the video signal from the logarithmic amplifier. An electromagnetic interference (EMI) meter was tuned to 20.4 MHz and used to measure the output of the 20.4 MHz IF amplifier in the FIM. This EMI meter pro-

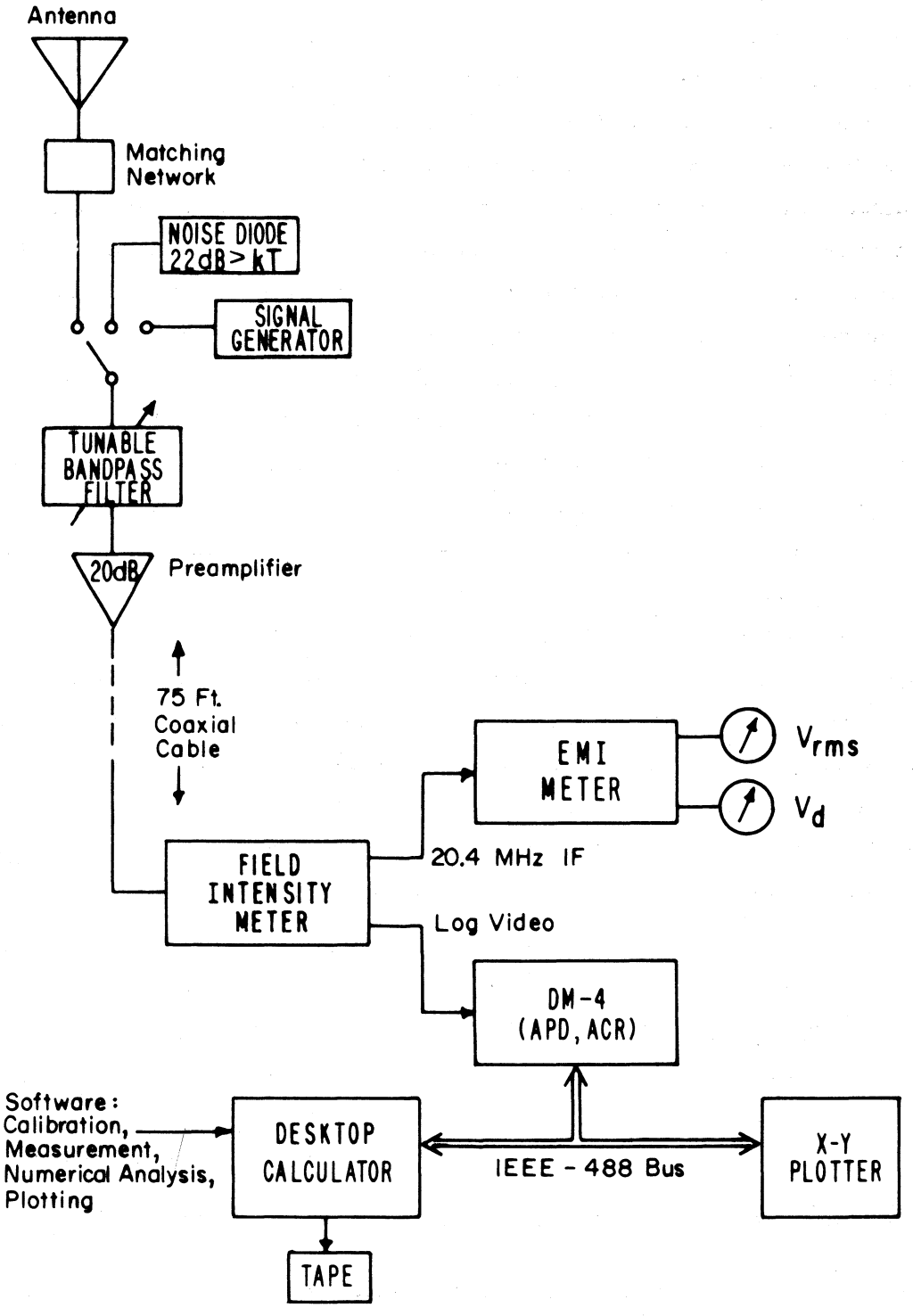

Figure 2 – Measurement Instrumentation

duced direct readings of rms voltage and Vd, to be compared with values of rms voltage and Vd computed from the APD's. Section 4 gives a definition of Vd and rms voltage. A separate report is being produced on this part of the experiment.* The logarithmic video output of the FIM was measured with a DM-4, giving APD's and ACR's. The DM-4 is an instrument designed to provide APD and ACR measurements when used with a logarithmic video output.** The DM-4 measured the noise at 31 levels, spaced approximate 3 dB apart.

The data from a 50-second measurement of APD's or ACR's was passed to the desktop calculator via an IEEE-488 bus connection. (It should be noted that it was found necessary to shut off the calculator during the actual measurements, to avoid contaminating the measurements with EM noise generated by the calculator). The desktop calculator processed the readings from the DM-4 in several ways according to software written by Falcon, G.D.***: 1) Calibration factors were added to the readings, converting measured millivolt levels into dBm at the antenna output. These calibration values had been measured earlier and recorded on a tape cartridge (see following paragraph on calibration). 2) The calibrated data were numerically integrated to get equivalent readings for several weighted averages, including rms, average, and average logarithm of the envelope voltage. The average and average logarithm were expressed in terms of their relationship to the rms,--Vd and Ld, respectively. See Section 4 for a specific definition. 3) Logistics information and labels were appended to the data. 4) All data and other information were recorded on a magnetic tape cartridge. Finally, 5) the data were plotted out on an IEEE-488 bus-controlled X-Y plotter, with appropriate labels and equivalent calculated weighted averages.

Table 1. Equipment Used in Measurements****

Field Intensity Meter	Ailtech NM37/57
EMI Meter	Ailtech NM-26T
DM-4	Prototype Built by NTIA
Desktop Calculator	Hewlett-Packard 9825
X-Y Plotter	Hewlett-Packard 9872A

*Ribbens, W., University of Michigan report under MVMA Project #1110. (To be published)

**Matheson, R.J., DM-4 Operation and Maintenance Manual. To be reported in an NTIA Technical Memorandum (unpublished).

***Falcon, G.D., Software for EM Noise Measurements Using DM-4 and 9825 Desktop Calculator. To be reported in an NTIA Technical Memorandum (unpublished).

****This list is not to be construed in any manner as a recommendation of this particular equipment. Rather, it is included here so that the reader can more thoroughly examine the experiment and derive a suitable estimate of the confidence to be placed in the measurement results.

The system was calibrated in several steps. The antennas were calibrated by the manufacturer who provided calibration tables with the antennas. These calibrations were checked and corrected, at the lower two frequencies, by measurements made under similar configurations to the actual noise measurements. Proximity effects from nearby cars and ground were of particular concern at the two lower frequencies. The system gain following the antenna output was checked with a noise diode at each frequency of interest. This measurement also provided a means of comparing the bandwidth of the measurement system with published data. The logarithmic amplifier slope factor was measured with a known CW signal amplitude set near the upper and lower amplitude ends of the log amplifier. Finally, a precision internal ramp generator was used to calibrate (in mV) each level of the DM-4. Calibration software combined these calibration procedures to give an equivalent dBm amplitude for each of the 31 DM-4 measurement levels, which were stored in the calculator and recorded on a magnetic tape cartridge. Preceding the measurements at a particular frequency, the appropriate calibration data tape file was loaded to calibrate that set of measurements. As a final check of proper calibration, an APD was made of noise from the noise diode as part of the normal measurement set. The computed rms value from the noise diode measurements was compared to a theoretical value, and the slope of the noise diode APD was checked to verify accurate system operation.

4. MEASURED DATA

Plots of the measured APD's and ACR's are shown in Figures 3 through 38. These plots are exact reproductions of the plots obtained during the measurements. The amplitude, in dBm, on these plots refers to the power at the antenna output terminal, plus a small system calibration factor (typically 1-2 dB). Factors needed to convert these values (in dBm) into field strength (in dB/1 μV/m) or antenna noise factors are given in chapter 5.

The noise diode measurement at 30.2 MHz (Figure 3) illustrates several features of APD's. The special scale used on the horizontal axis causes detected Gaussian noise to be plotted as a straight line with a slope of $-\frac{1}{2}$. The fact that the lower amplitude portions of most of the APD measurement in other figures have a slope of $-\frac{1}{2}$ suggests that the lower amplitude portion of these noise measurements are like Gaussian noise. In fact, since the lower amplitude portion of the noise measurements coincides with the APD of the measurement system noise (not included in this report), it is very likely that the low

amplitude portion of the noise measurements was simply measurement system noise covering up the actual external noise. The slight curvature at the lowest end of some APD measurements is caused by a non-ideal performance of the FIM logarithmic amplifier at very low amplitudes.

Three weighted averages have been calculated from the APD measurements and are displayed near the lower left-hand corner of the graph. The rms average (in dBm) gives the integrated average power of the noise. Based on a 10 kHz receiver bandpass and an excess noise of 22 dB>kT, the rms reading should be -112 dBm. The V_d reading is a dB ratio of the rms voltage to the average voltage; for a theoretical Gaussian signal V_d = 1.049 dB. L_d is the dB ratio between the rms and the average logarithm; for a Gaussian signal, L_d = 2.493 dB. The close agreement of measured values with these theoretical values is a convincing argument that system calibration has been done accurately.

Measurements were made at 5 frequencies between 30.2 MHz and 445 MHz. APD's were measured at all of these frequencies, only the background, the 12-car matrix, and the super-noisy vehicle (SNV) are reproduced in this report. Other measurements were made for calibration and diagnostic purposes and are not included here. In addition to the APD measurement, ACR's were measured for 30 MHz. It was initially intended to include ACR measurements for all frequencies, but a malfunction of the DM-4 prevented reliable ACR data from being obtained for the later (higher) frequencies.

Figure 10 shows an ACR measurement of background noise at 30 MHz. This is a typical graph of Gaussian noise. Notice that the maximum value of ACR (5500) occurs about at the 50% point of the corresponding APD from Figure 3. Decreasing amplitude gives fewer crossings because the signal gets below that amplitude a fewer number of times. Similarly, increasing amplitude gives fewer crossings since the signal gets above that amplitude a fewer number of times. The horizontal scale is plotted on a logarithmic scale, with the decades marked by 10^n, i.e., 10^3 means 1000 crossings/sec, 10^4 means 10,000 crossings/sec, etc. On the other measurements of average crossing rate (Figures 11 through 14) one can see that the major departures from the background curve of Figure 10 occur at the same amplitude ranges where the corresponding APD's depart from the APD background.

The ACR data in Figure 13 may be partly in error and is typical of later DM-4 malfunctions. The maximum ACR for Gaussian noise is too high. However, the portion of the ACR measurement above -110 dBm is probably correct, based on instrumentation tests made later.

Figure 4 was made during a period in which two very short power outages occurred, and the data is surely subject to interpretation. However, since these data were not used directly anywhere in the report, no effort was made to repeat the measurement.

5. DATA SUMMARY AND CONCLUSIONS

This section contains a summary of all of the measurements made, using the calculated rms value of the noise. Although the rms value is only a single point used to characterize the whole APD--and, therefore, must necessarily be a somewhat incomplete characterization--the rms value is a measure of the total energy radiated at each frequency and is probably the most significant single parameter which describes the noise.

The amplitude scale on the preceding APD and ACR graphs is plotted in dBm at the receiving antenna terminals. The rms values from the APD Figures are recorded in the 4th column of Table 2 and represent the rms power in a 10 kHz bandwidth at the antenna terminals. The amount of energy in the electromagnetic field near the measurement antenna can be calculated only by making several assumptions. First, one must know the gain of the antenna (or some equivalent "antenna factor") at each frequency of measurement. Although the gain of the antenna may be measured, more critical assumptions must be made about the directional qualities with which the noise is radiated from the cars and the relationship between the electric and the magnetic componants of the noise in the near field. Neither of these questions was considered in this set of measurements. There was no effort to locate maximum or minimum levels of noise by moving the measurement antenna to different sites near the cars. In addition, there was no attempt made to measure the energy in the magnetic field of the noise. Since the measurement antenna was in the near field of the cars at the lowest two frequencies (where there is no fixed ratio between the energy in the electric and magnetic fields), it is possible that substantial measurement inaccuracies may have resulted.

Nevertheless, lacking sufficient data to make a more precise conversion, the following assumptions were made: 1) Antenna gains were measured at the two lowest frequencies, because it was felt that there might be substantial "proximity" effects from the cars and the ground at the lower frequencies. 2) For the highest three frequencies, the antenna factors supplied by the antenna manufacturer were used in the calculations. 3) In all cases, it was assumed

that the electric and the magnetic field components had the same relation as in a far-field measurement.

The fifth column of Table 2 contains an antenna factor, K1, which can be added to the rms level at the antenna terminal to give the rms field strength in dB above 1 microvolt. The sixth column of the table shows the measurements converted to rms field strength (in decibels above a microvolt/meter for a 10 kHz bandwidth).

The seventh column of Table 2 contains a factor, K2, which may be used to convert field strength to F_a, the effective antenna noise figure. F_a--given in the eighth column--is described more fully in the references and is generally most useful in calculations of system sensitivity (Spaulding, 1976). The formula used here,

$$F_a = E_n - 20 \log f_{MHz} - 10 \log b + 98.9,$$

is for an ideal quarter-wave dipole (Lauber, 1977). E_n is field strength (in dB>1μV/m) and b is bandwidth (in Hz). Other antenna types will require different conversion formulas.

In Figure 39, F_a is plotted as a function of frequency for the horizontal and vertical polarization antenna orientations with each of the two test configurations. The measurements made under identical sets of operating conditions have been joined, implying a relatively smooth curve joining the measured points. This may not be actually true; relatively large excursions might be found between the few points which actually were measured, caused by resonances at particular frequencies in the ignition systems.

Underneath the four sets of graphed data is a dashed line representing a background level of galactic noise. From the standpoint of noise being a problem to communications systems, it probably doesn't matter too much as long as noise remains below the galactic noise level. Galactic noise will remain relatively constant at the indicated level, furnishing an approximate lower limit to systems operating with low gain antennas. On the other hand, these measurements show that the cars were causing noise well in excess of galactic noise levels. Furthermore, the noise from the cars was very impulsive, causing occasional noise spikes which were very much higher than the Gaussian noise levels from galactic noise.

Finally, this set of measurements is a very limited set, and it would be ill-advised to conclude that these measurements describe a "typical" set of cars. Although the overall measurement accuracy at the antenna terminals is estimated to be within $\pm$ 2 dB, the variations in level arising from the selection of cars and in the orientation of the measurement antenna with respect to those cars is believed to be considerably larger than the bounds on measurement accuracy. Therefore, this set of measurements should be regarded as a single data point to be considered along with other measurement sets--withholding judgement until enough data has been measured that a pattern becomes visible.

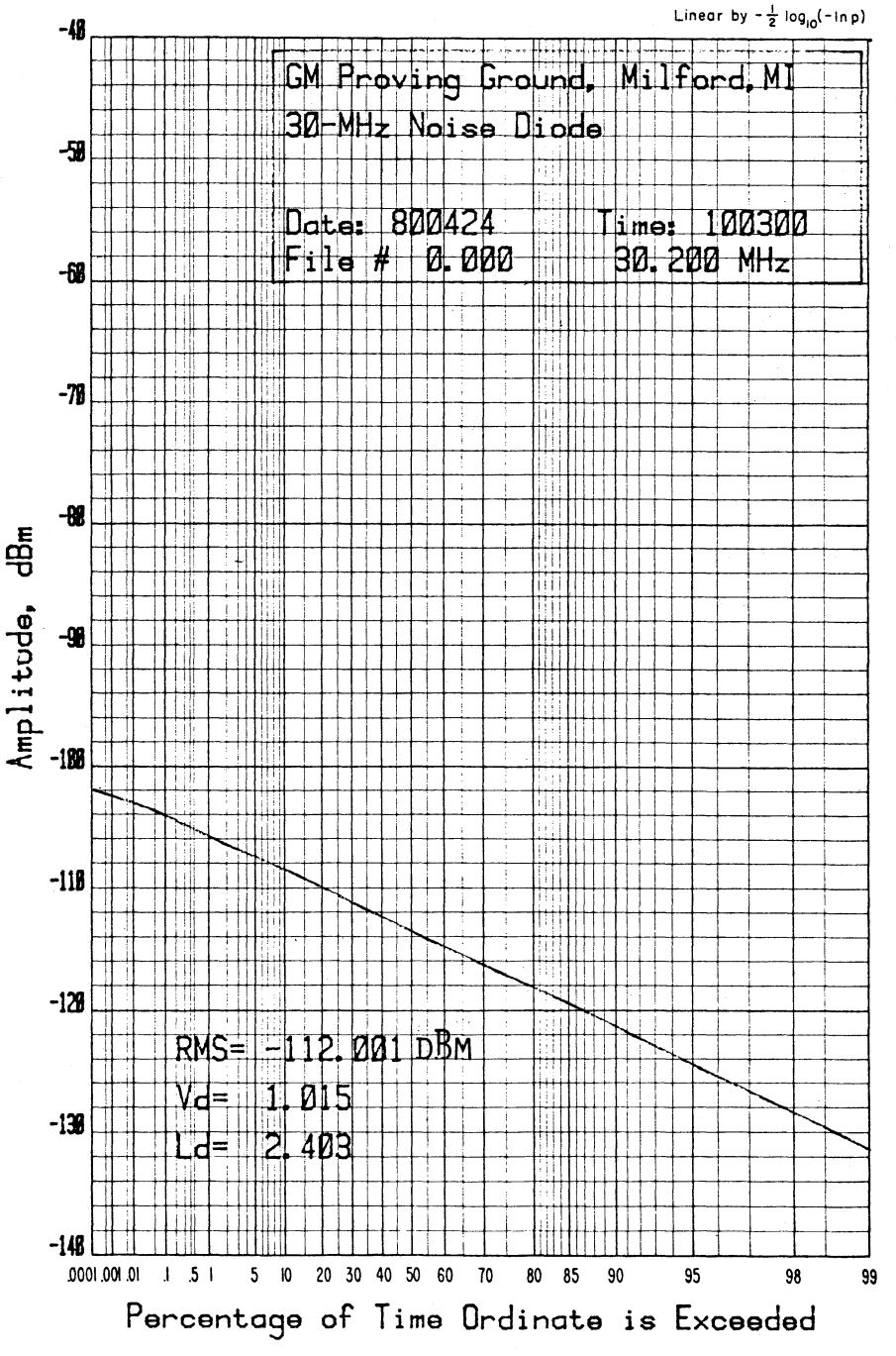

Figure 3. APD 30 MHz Noise Diode

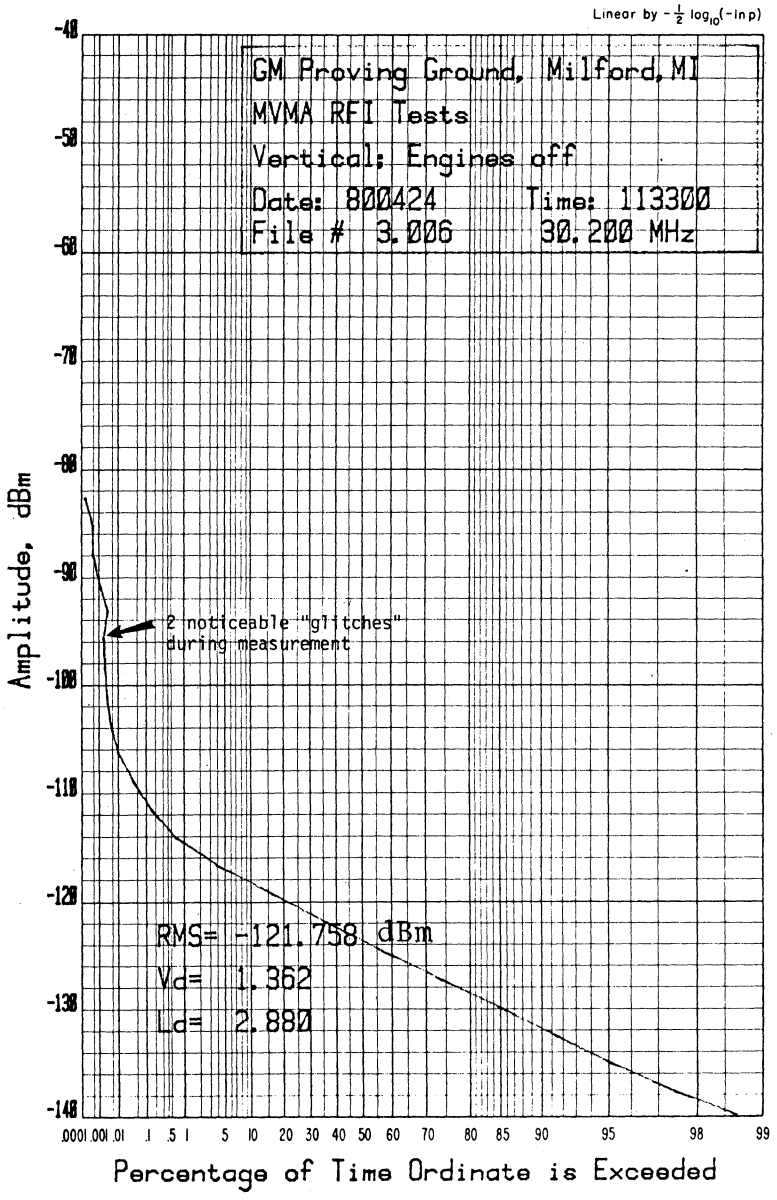

Figure 4. APD 30 MHz Background

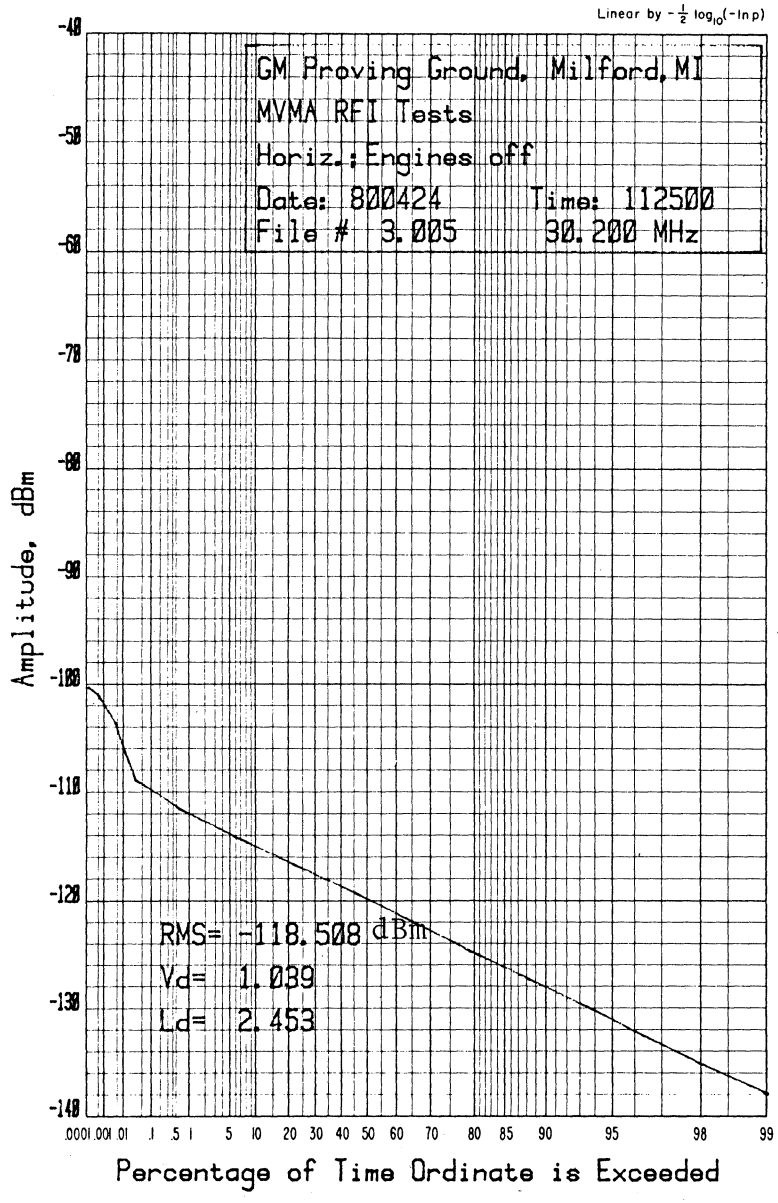

Figure 5. APD 30 MHz Background

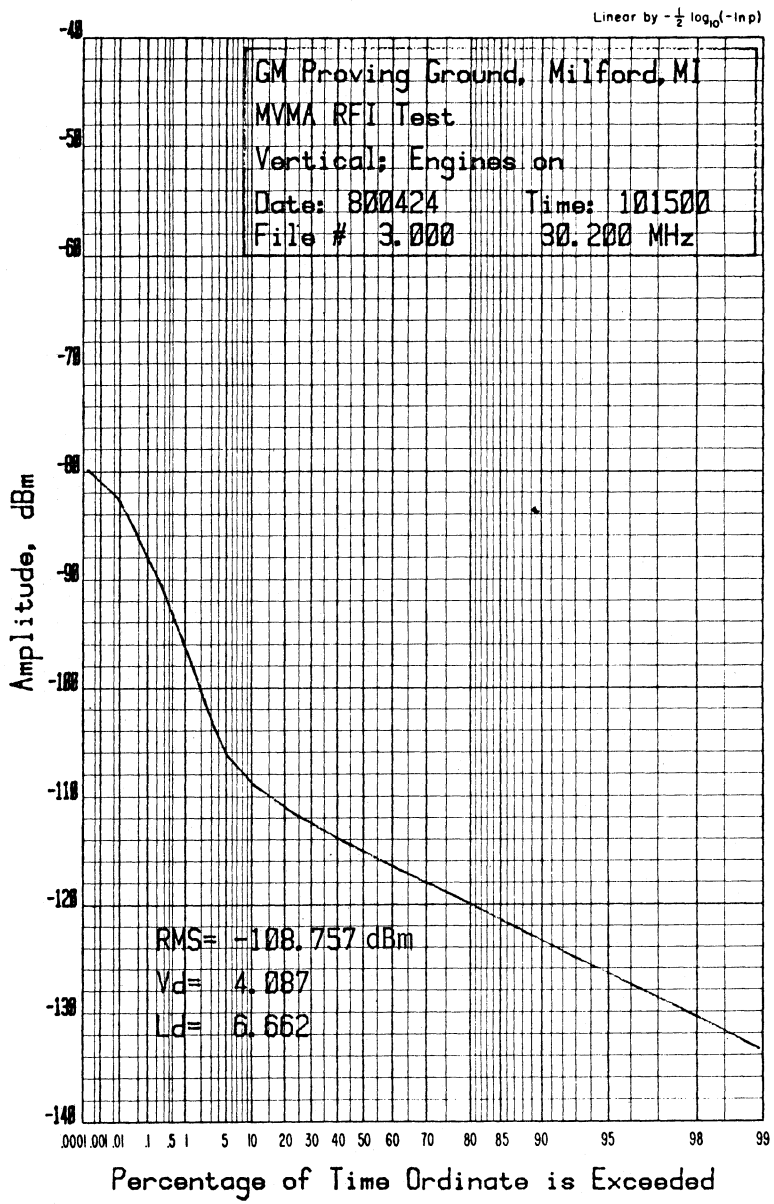

Figure 6. APD 30 MHz 12 Car Matrix

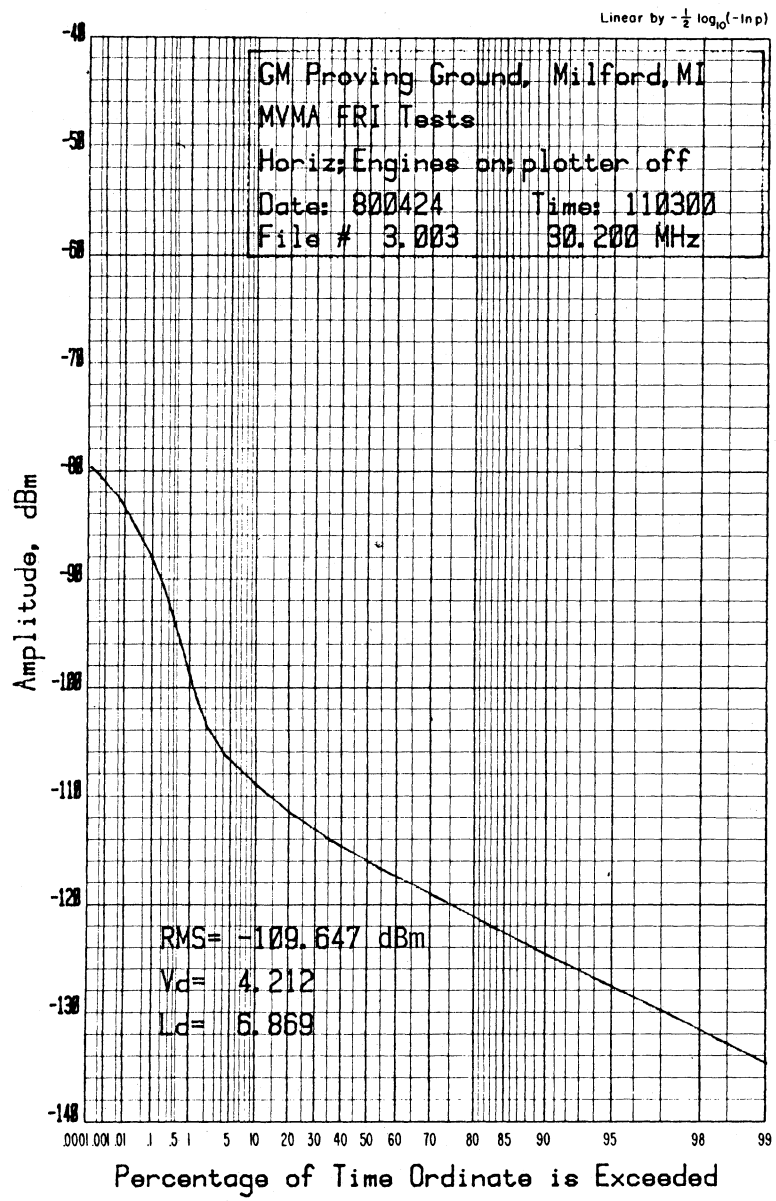

Figure 7. APD 30 MHz 12 Car Matrix

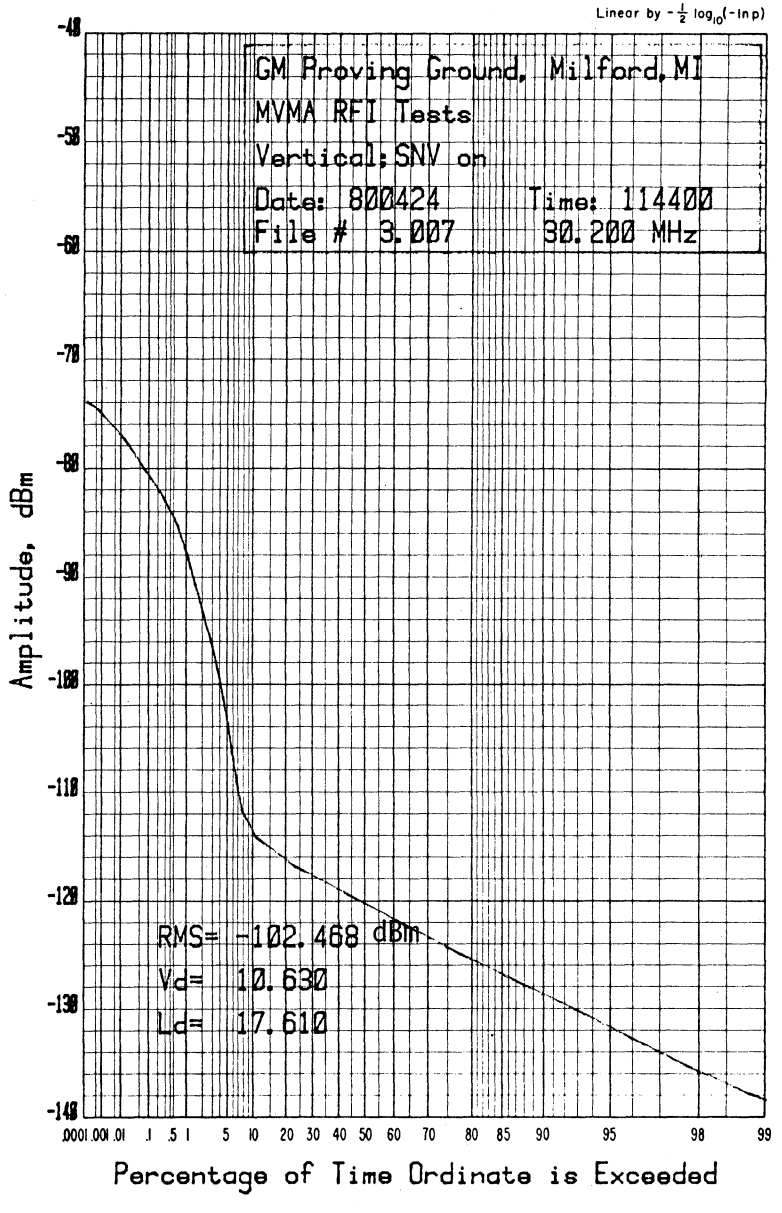

Figure 8. APD 30 MHz SNV

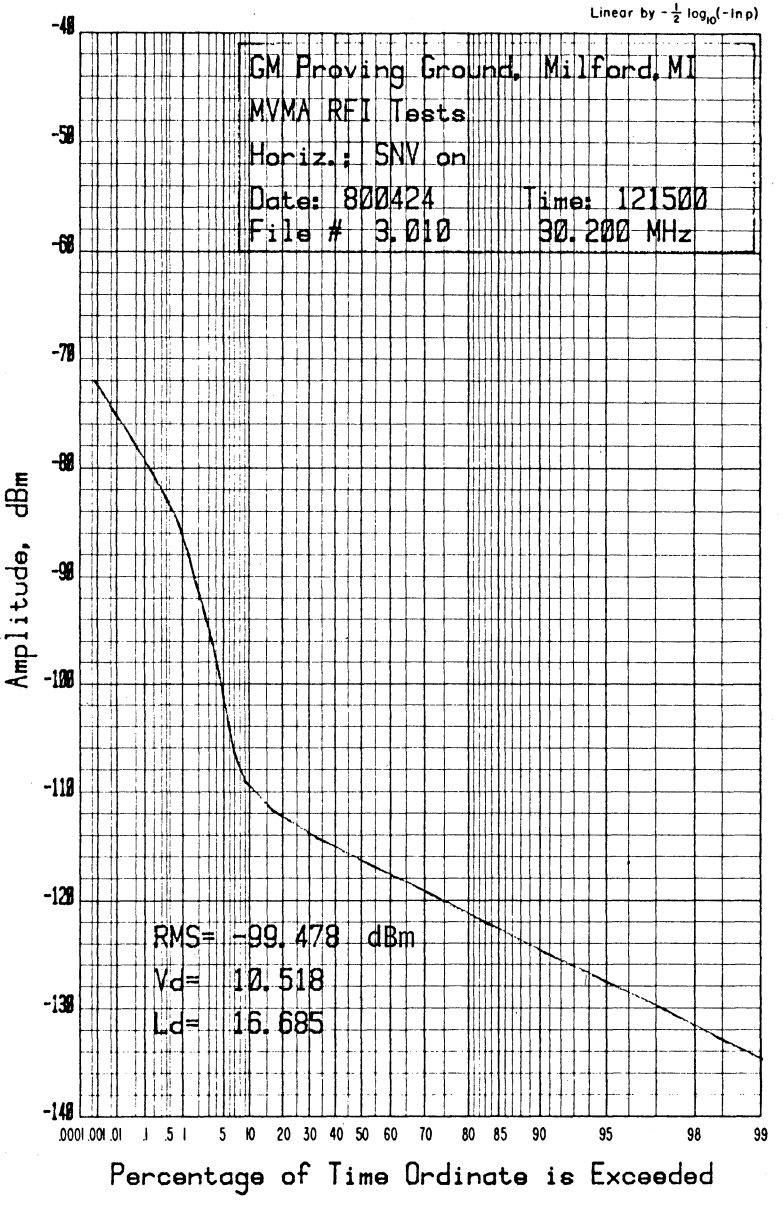

Figure 9. APD 30 MHz SNV

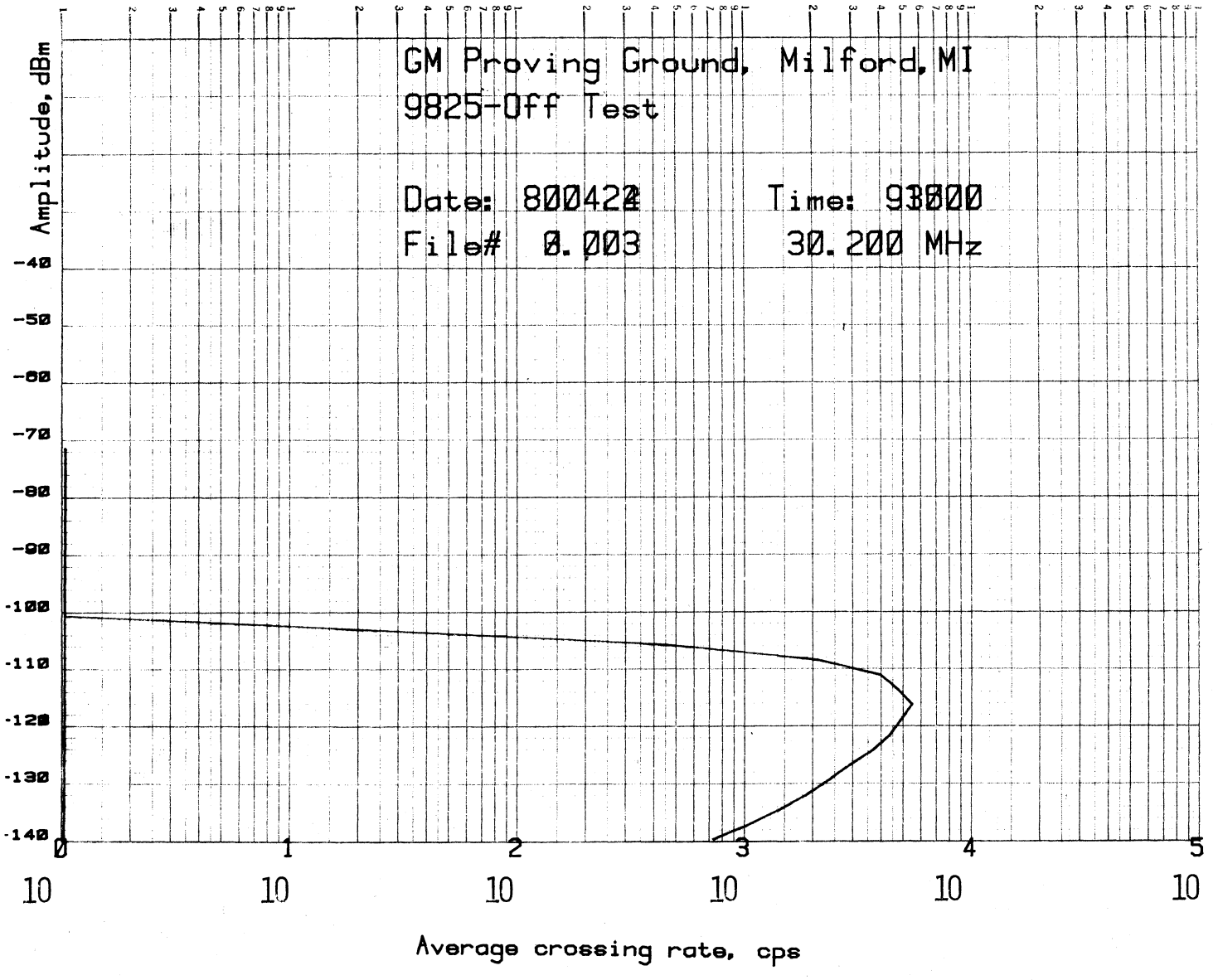

Figure 10. ACR, 30 MHz - Background

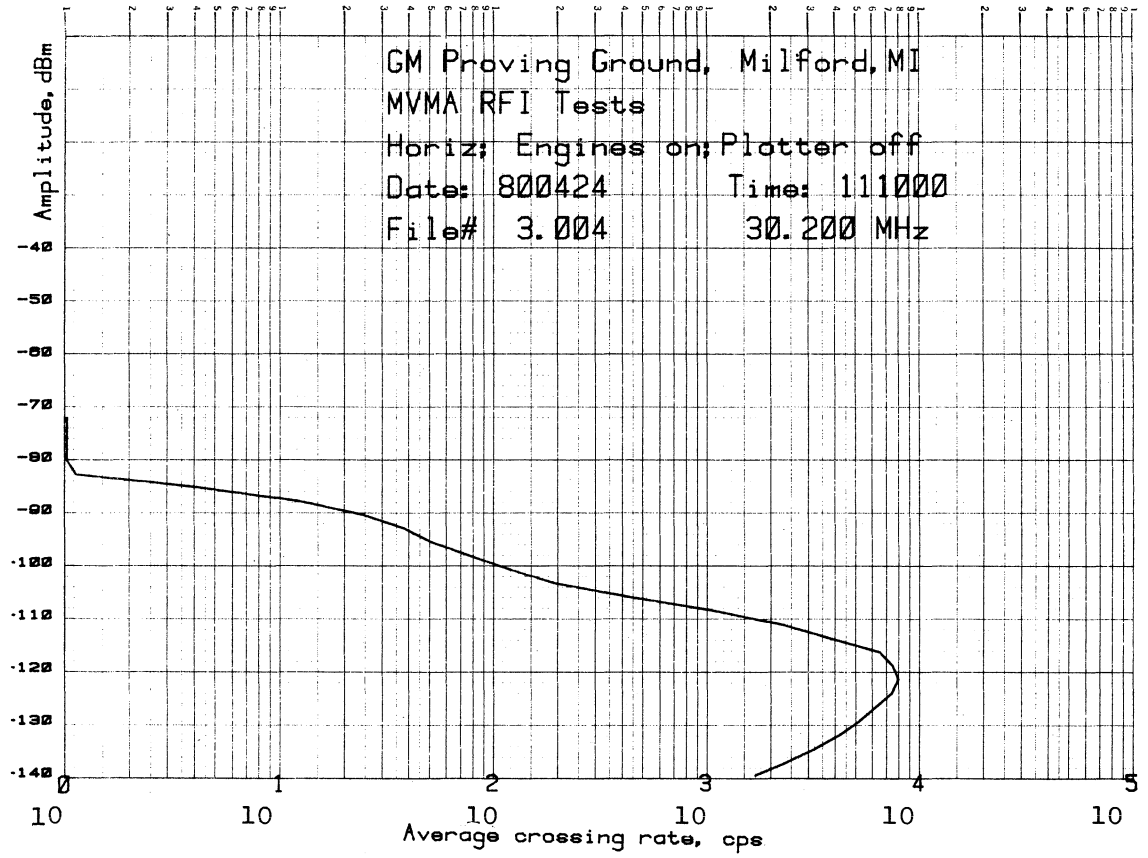

Figure 11. ACR, 30 MHz - 12 Car Matrix

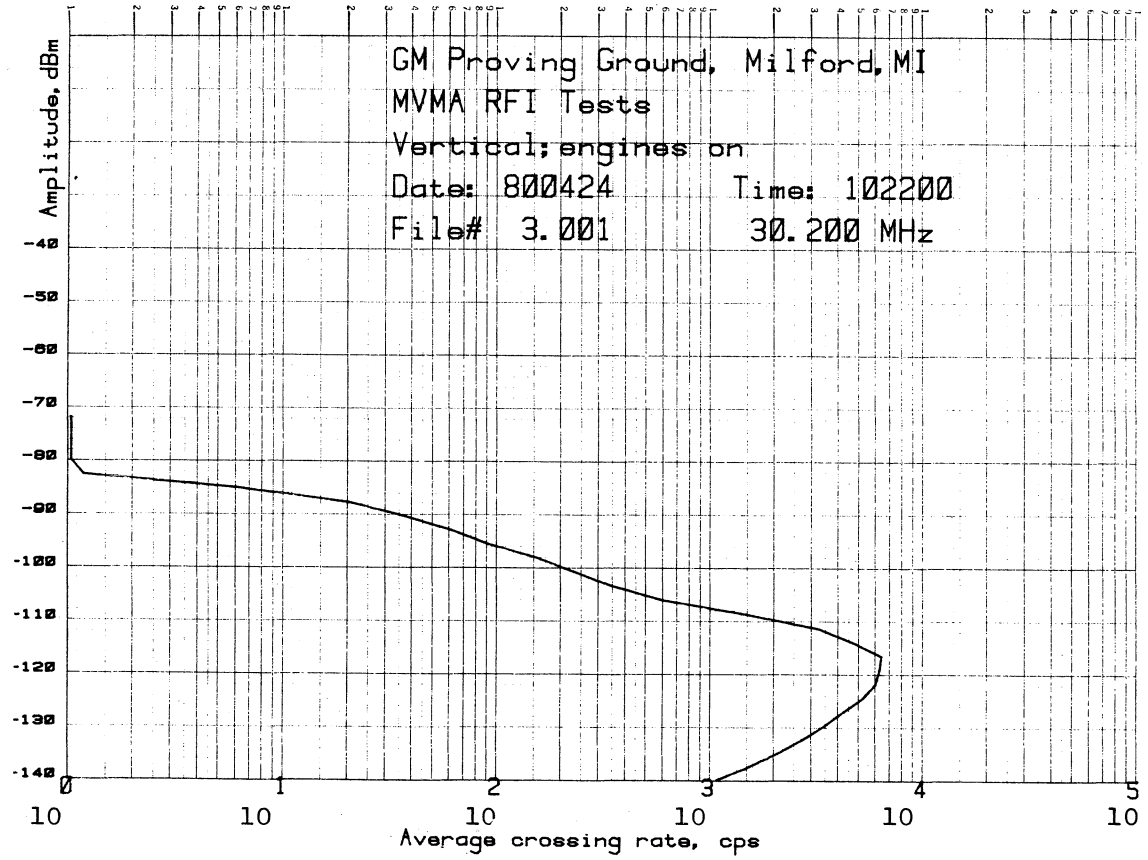

Figure 12. ACR, 30 MHz - 12 Car Matrix

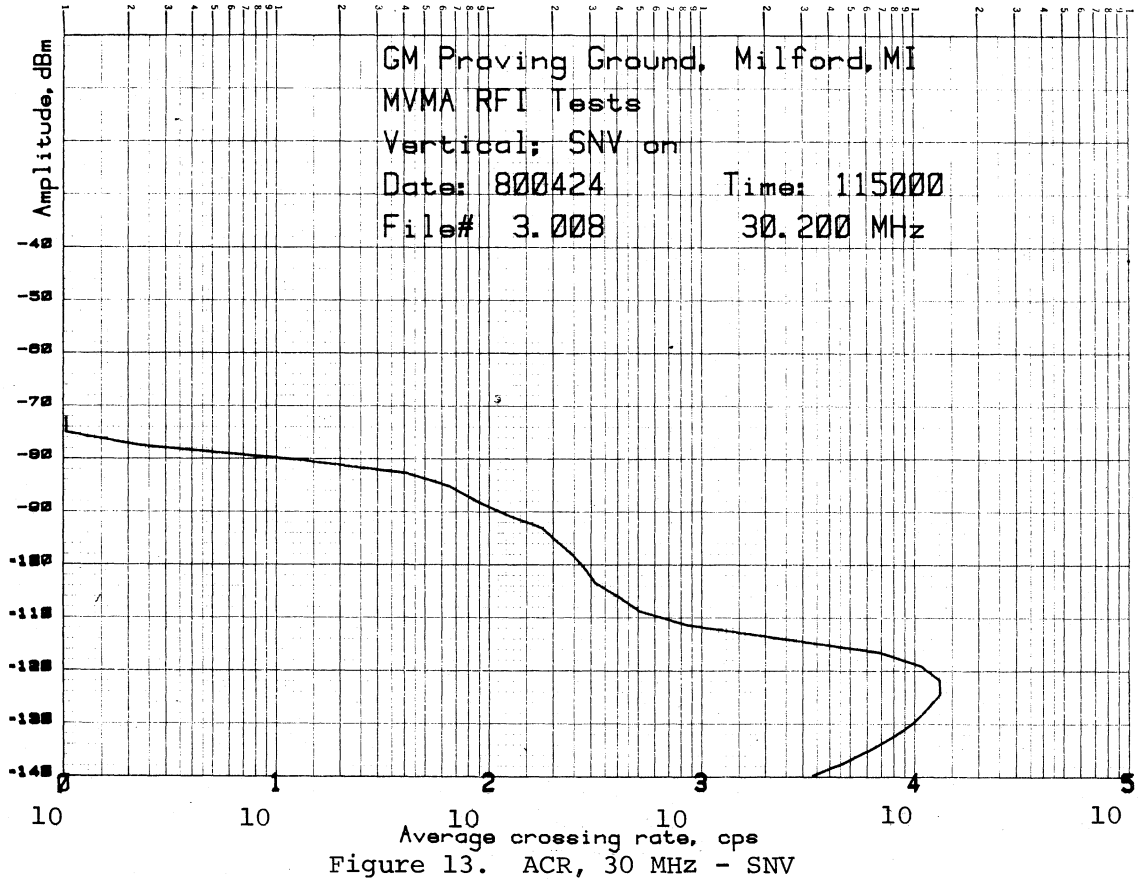

Figure 13. ACR, 30 MHz - SNV

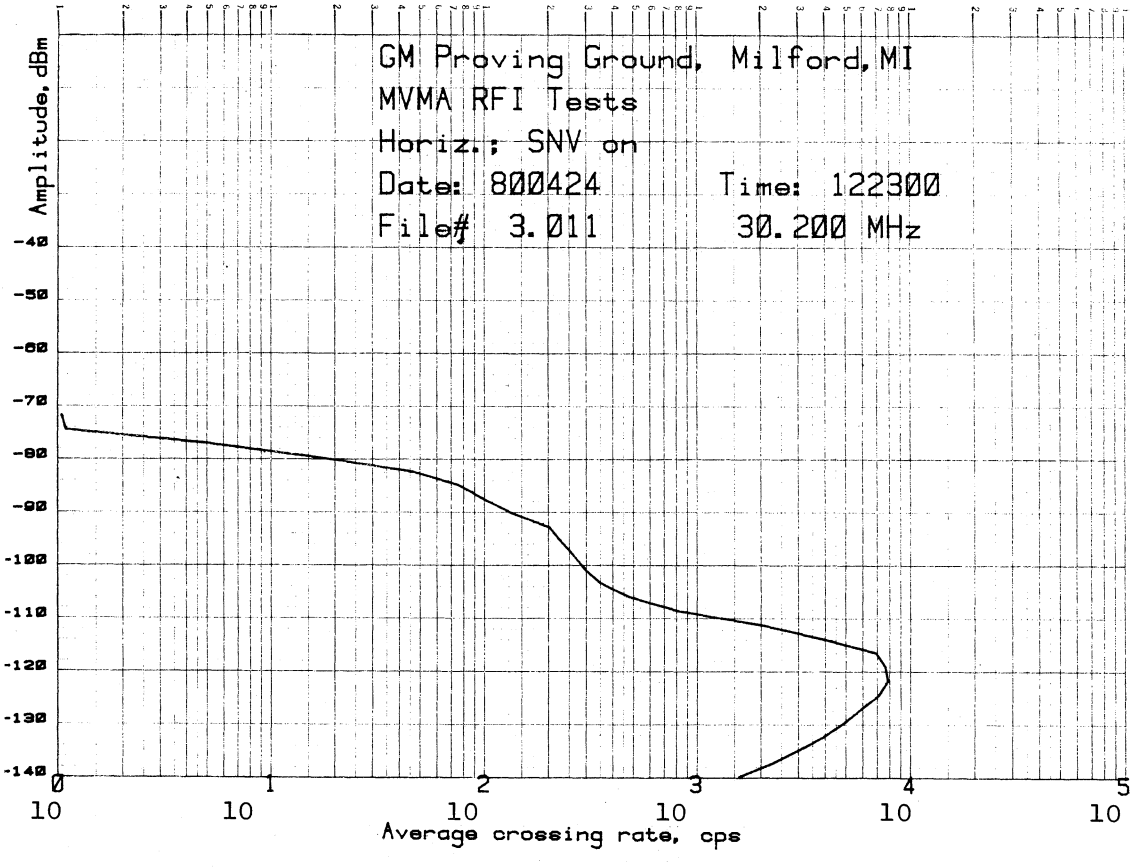

Figure 14. ACR, 30 MHz - SNV

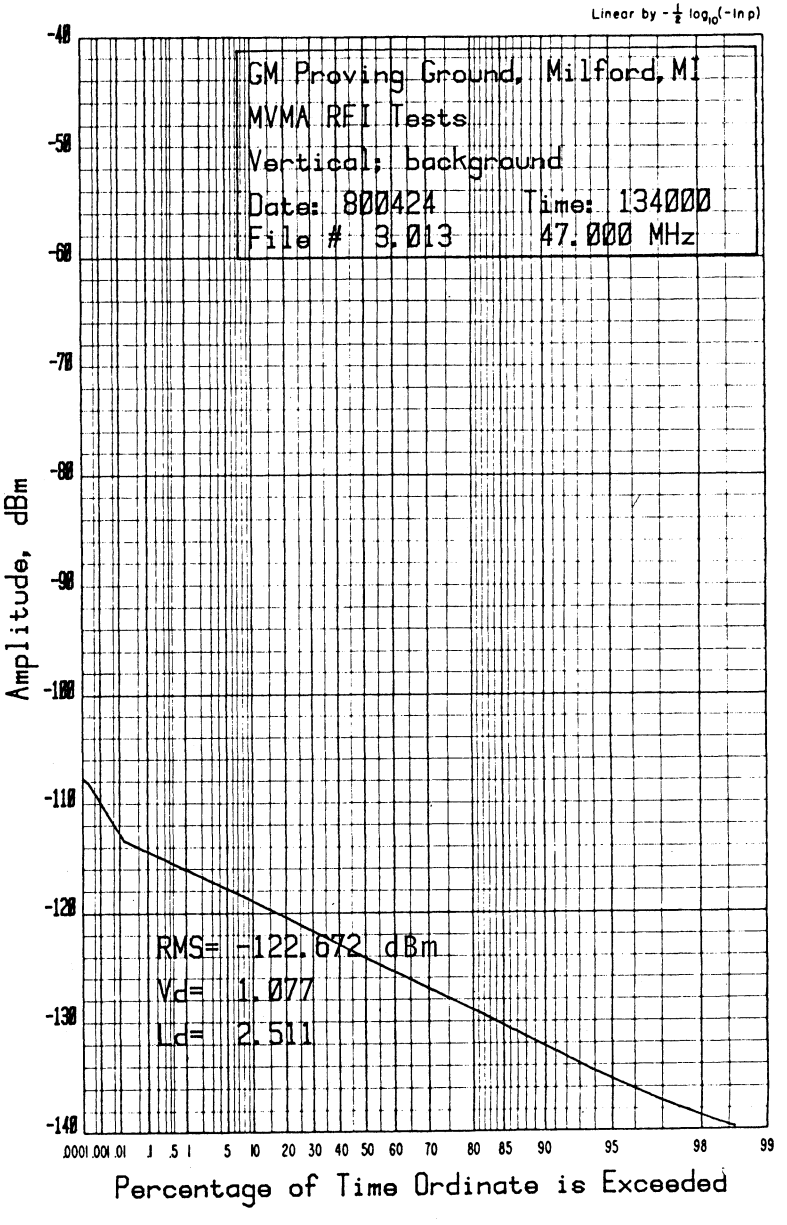

Figure 15. APD, 47 MHz - Background

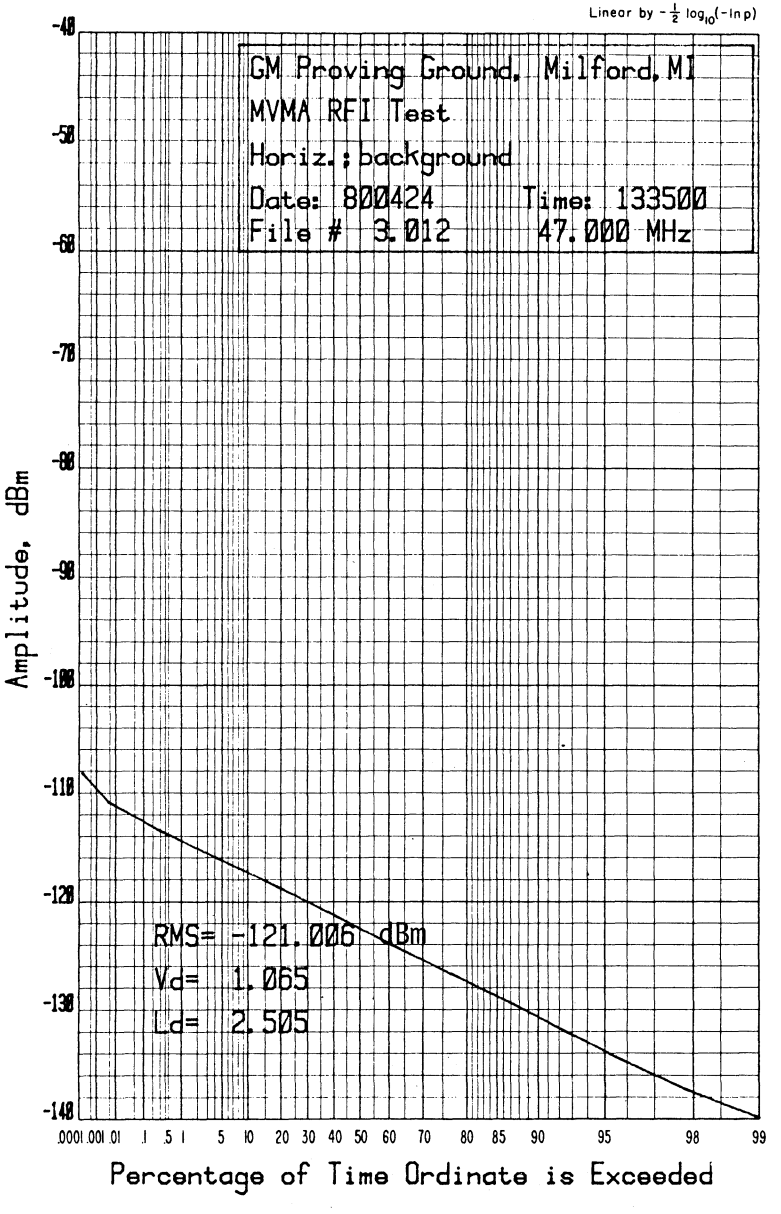

Figure 16. APD, 47 MHz - Background

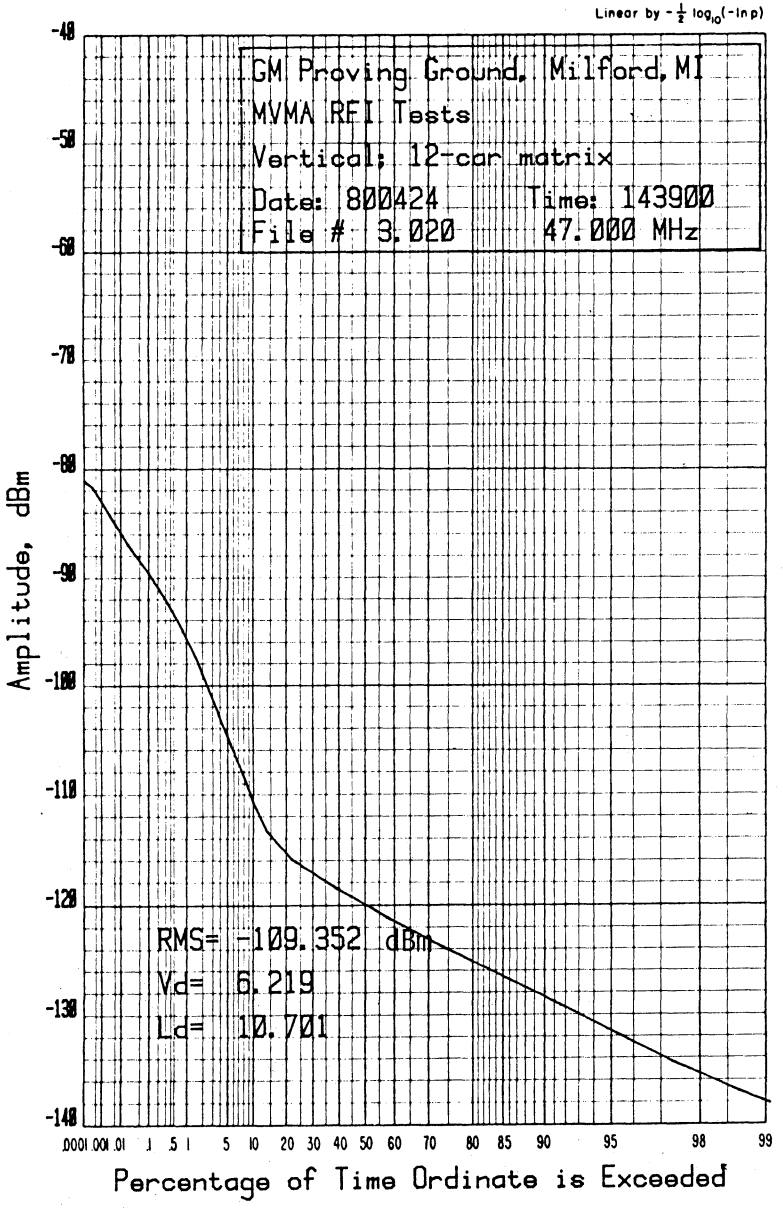

Figure 17. APD, 47 MHz - 12 Car Matrix

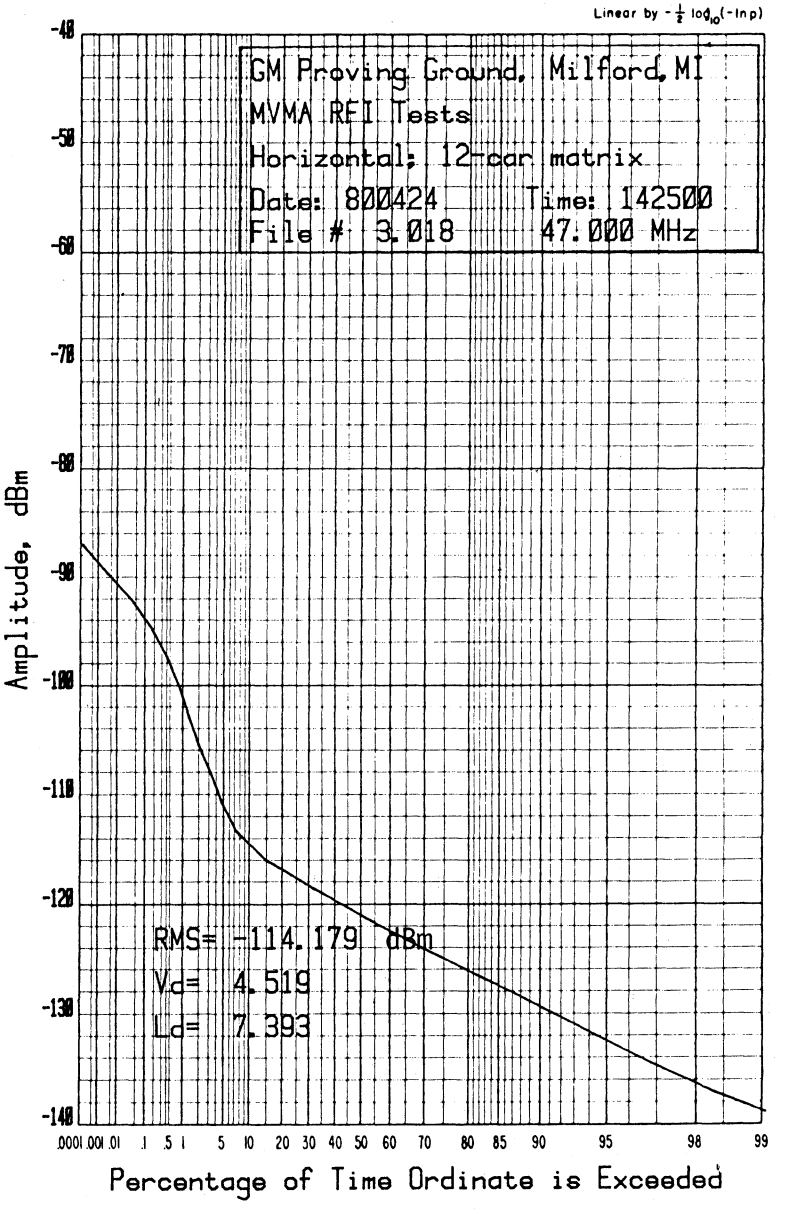

Figure 18. APD, 47 MHz - 12 Car Matrix

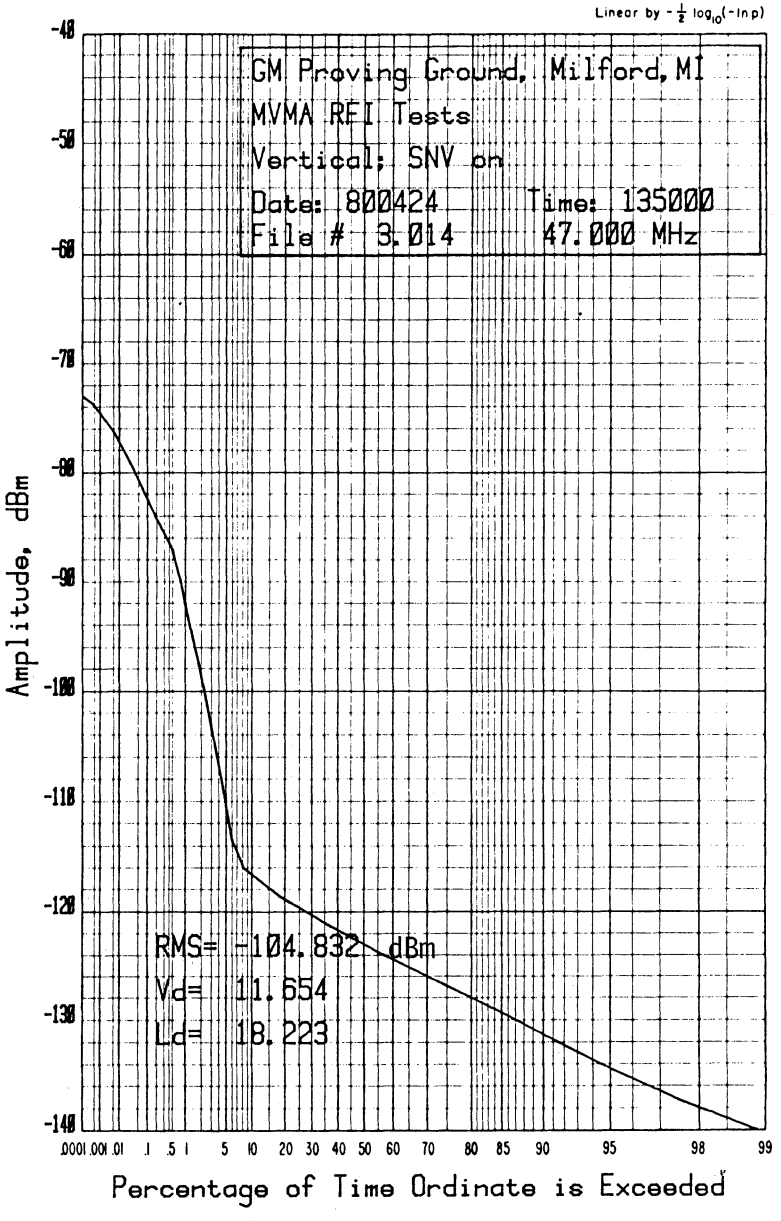

Figure 19. APD, 47 MHz - SNV

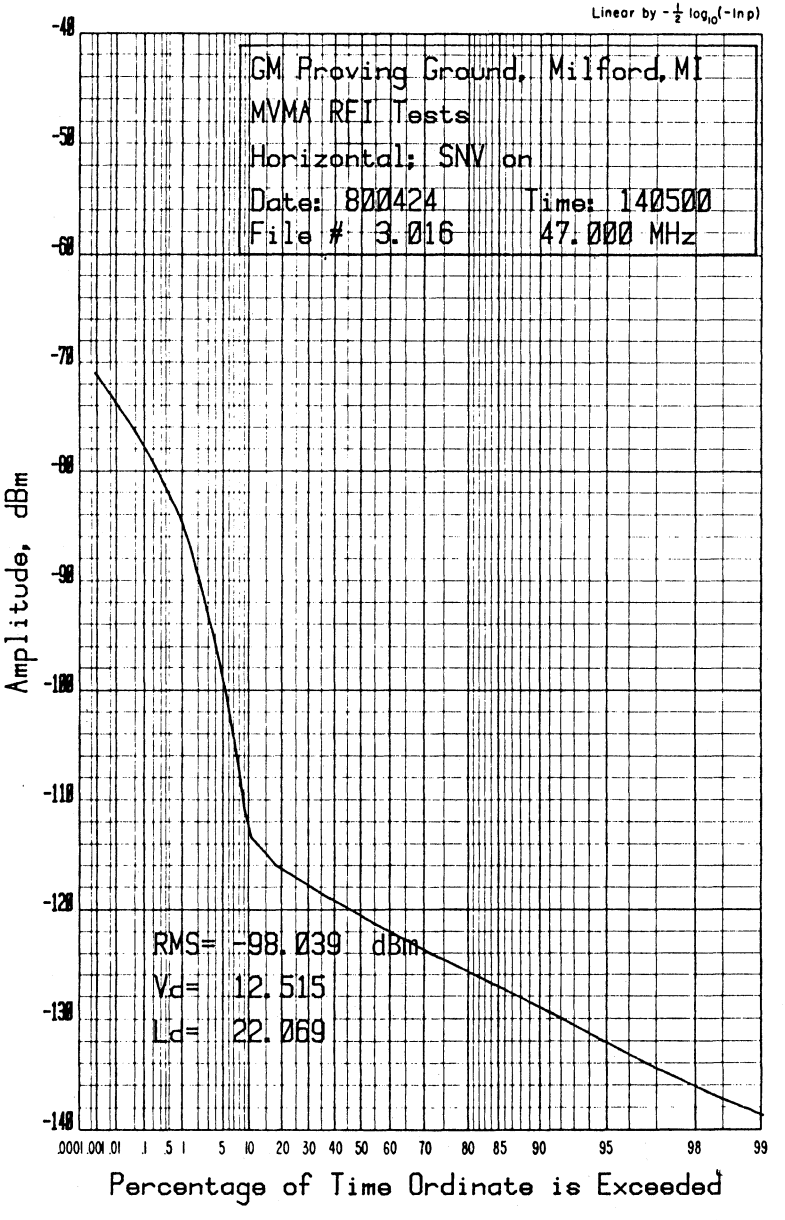

Figure 20. APD, 47 MHz - SNV

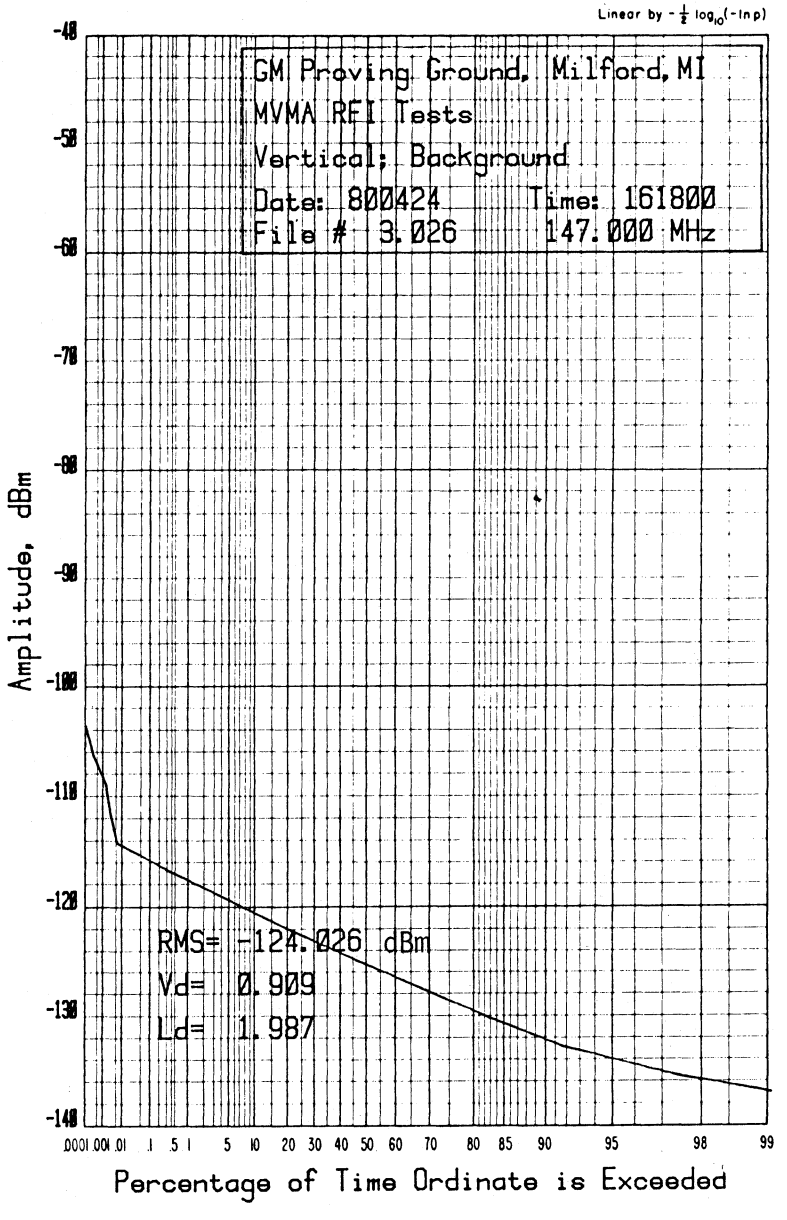

Figure 21. APD, 147 MHz - Background

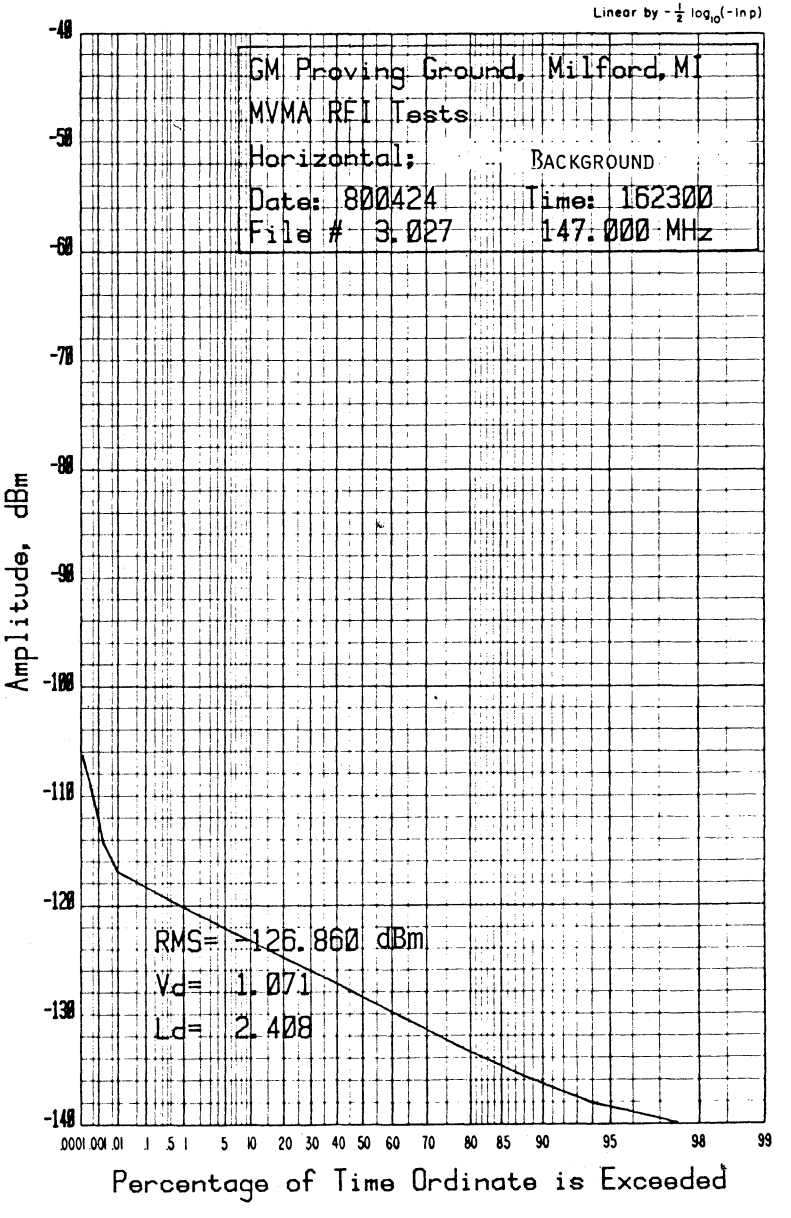

Figure 22. APD, 147 MHz - Background

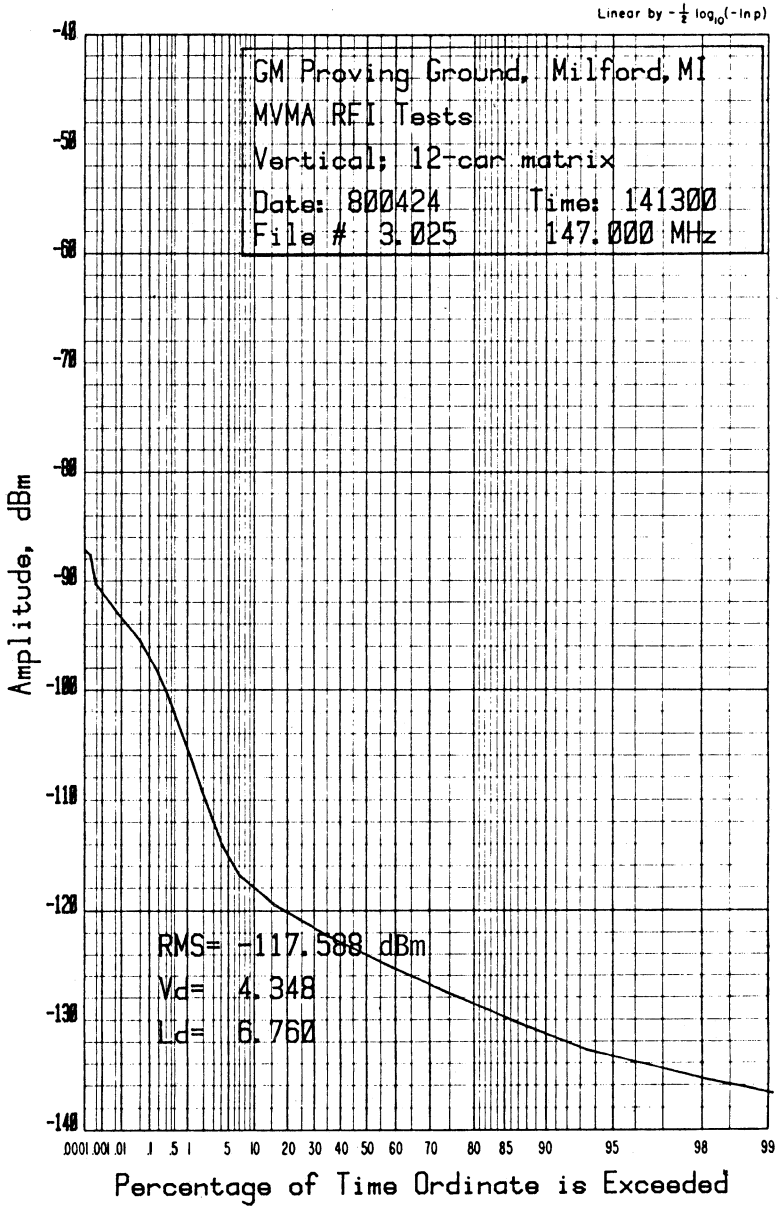

Figure 23. APD, 147 MHz - 12 Car Matrix

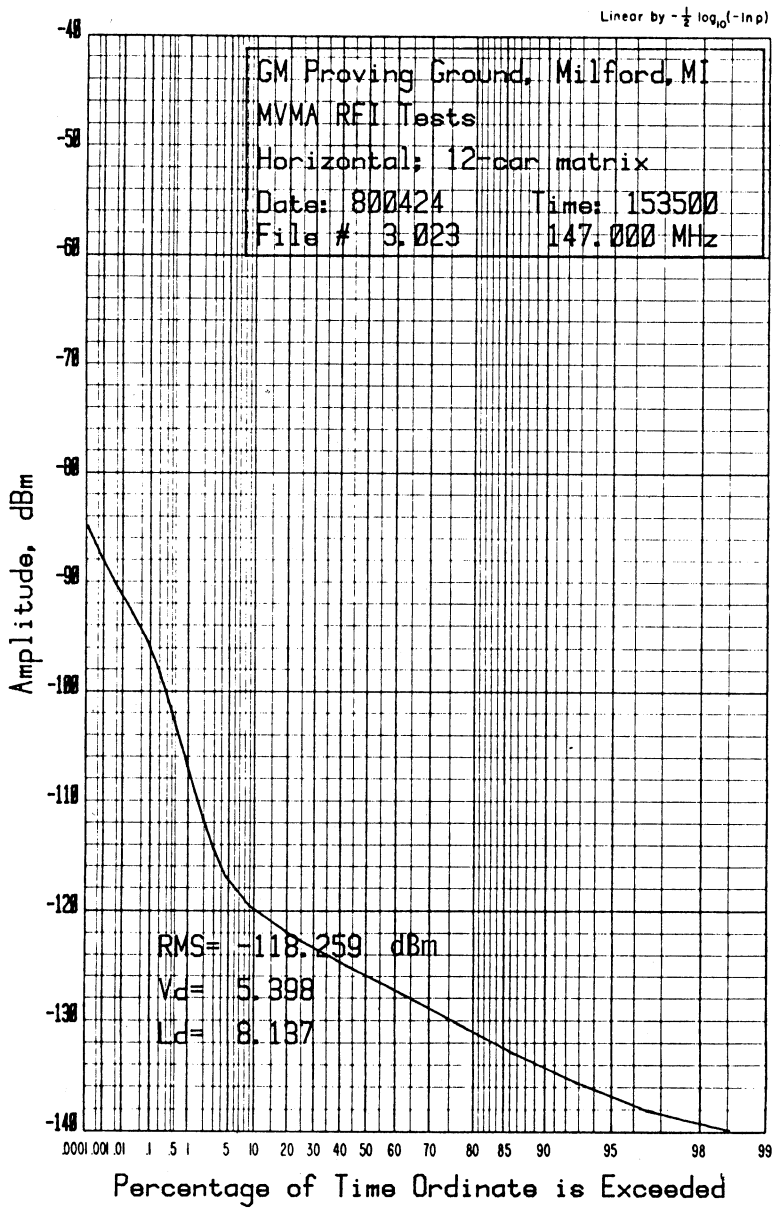

Figure 24. APD, 147 MHz - 12 Car Matrix

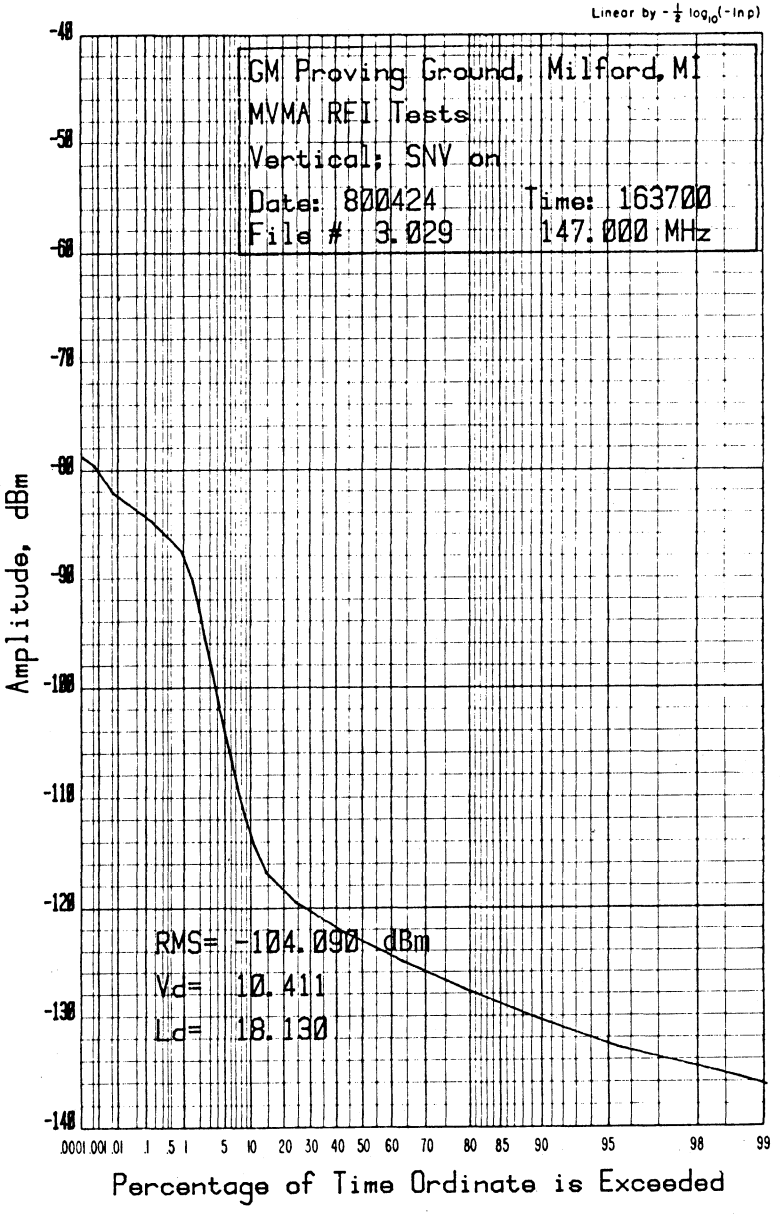

Figure 25. APD, 147 MHz - SNV

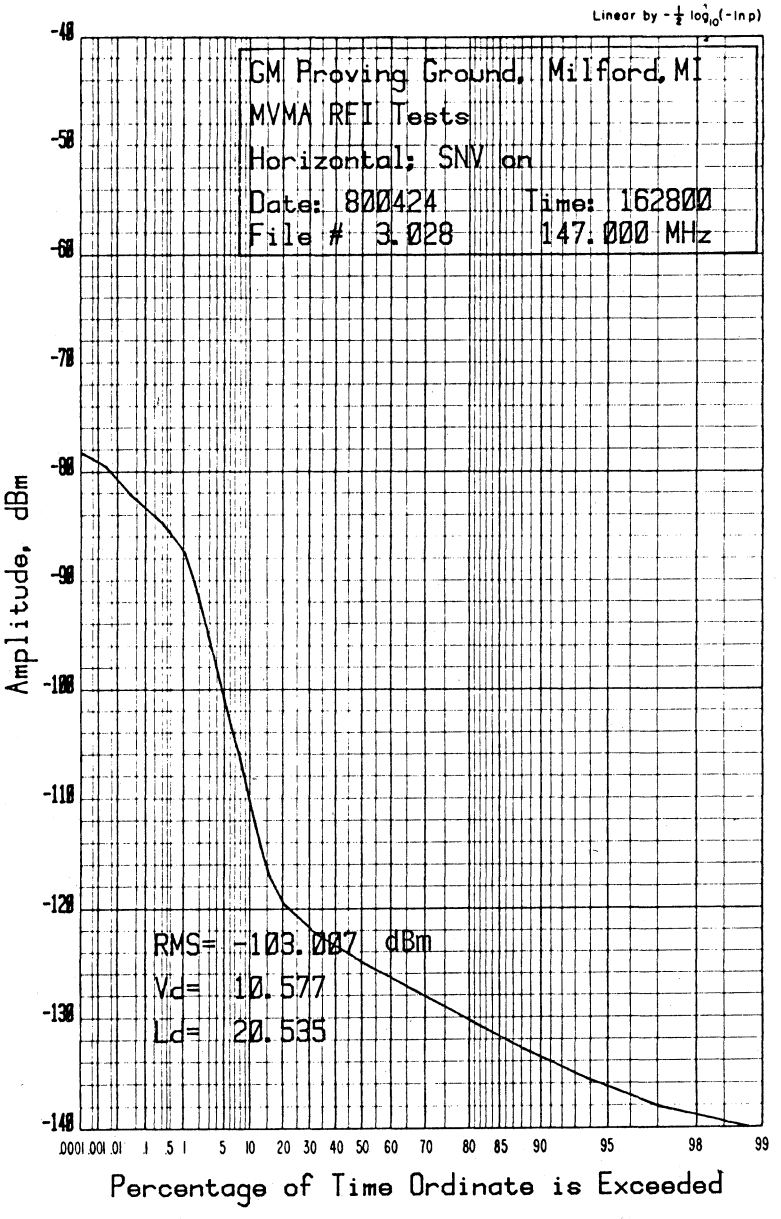

Figure 26. APD, 147 MHz - SNV

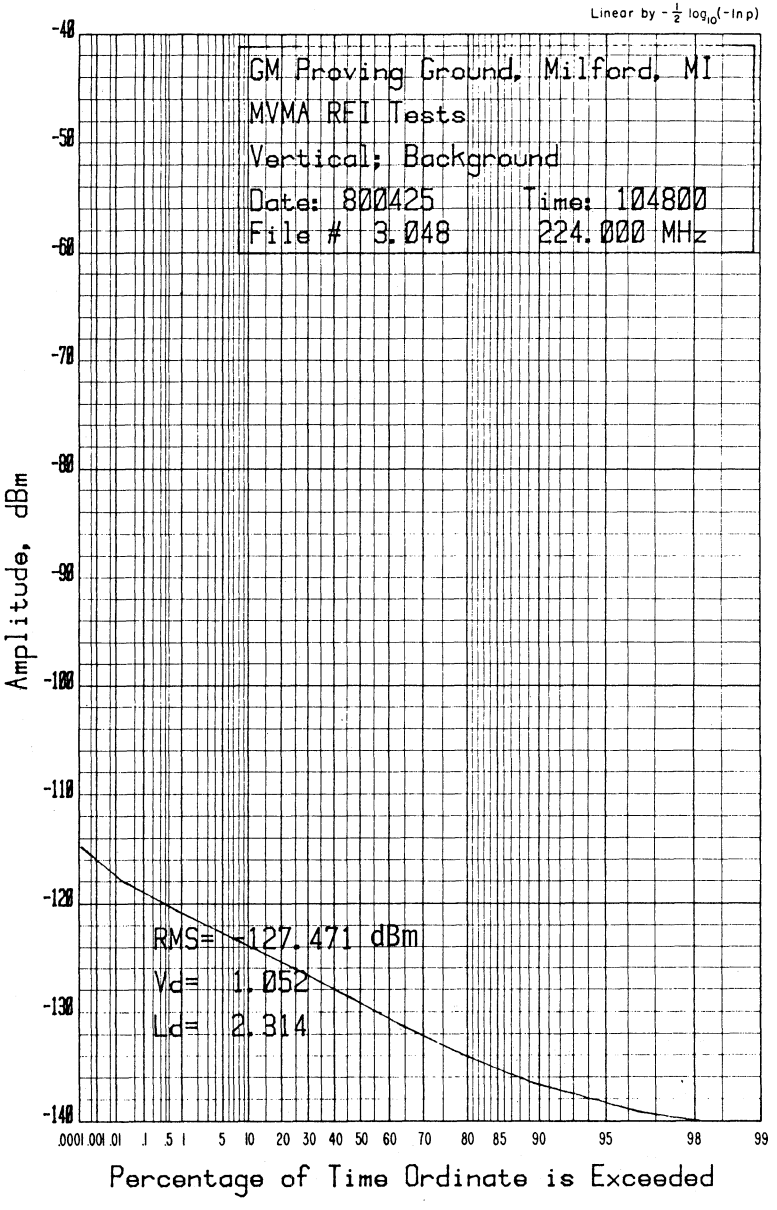

Figure 27. APD, 224 MHz - Background

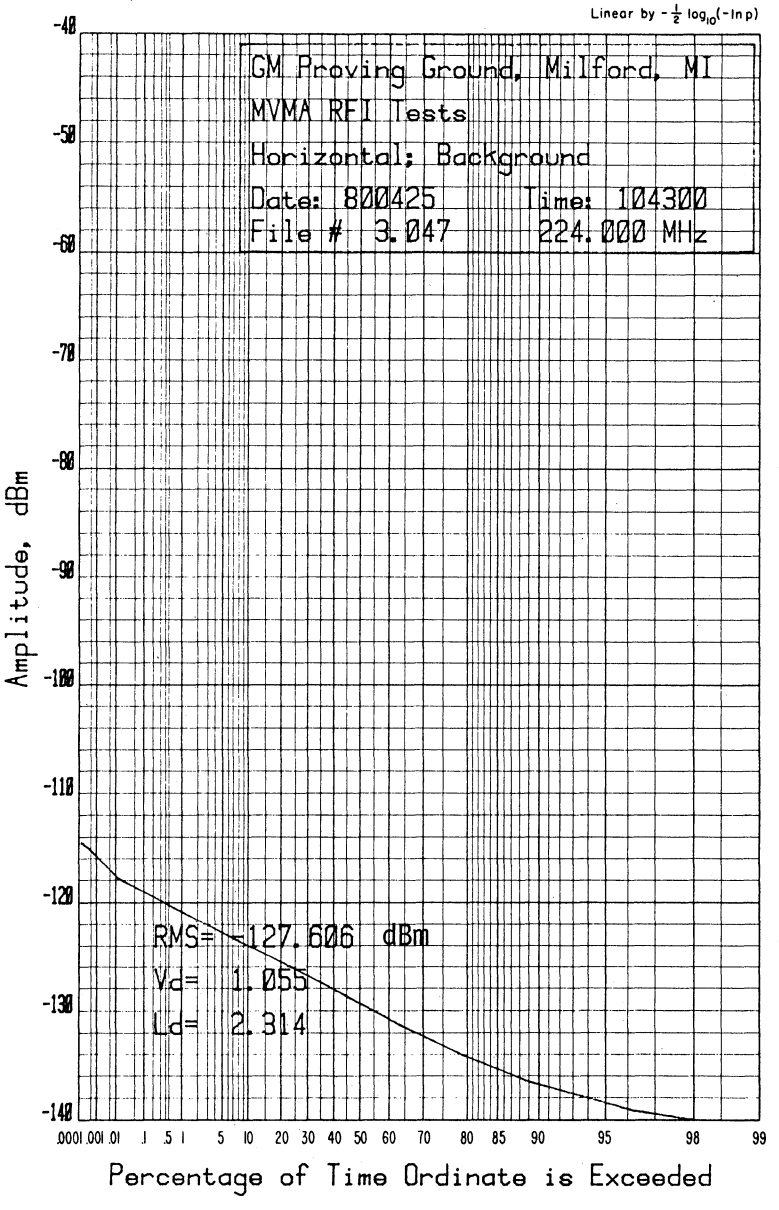

Figure 28. APD, 224 MHz - Background

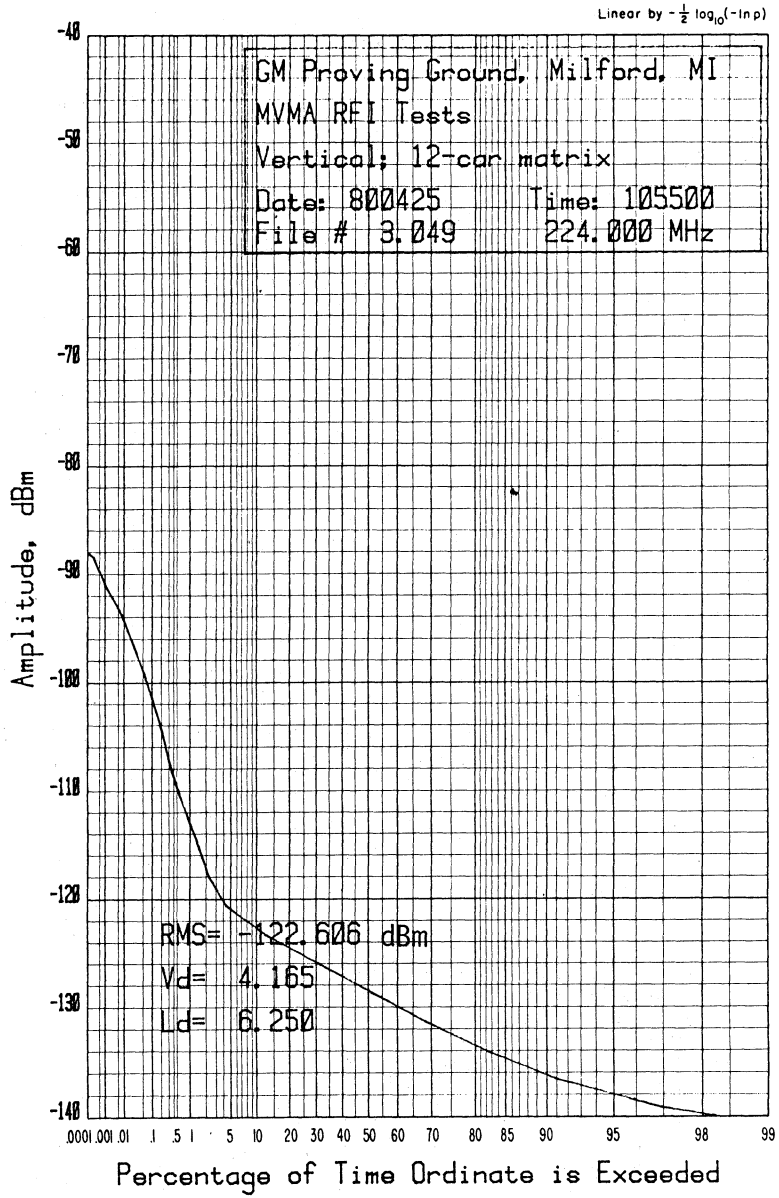

Figure 29. APD, 224 MHz - 12 Car Matrix

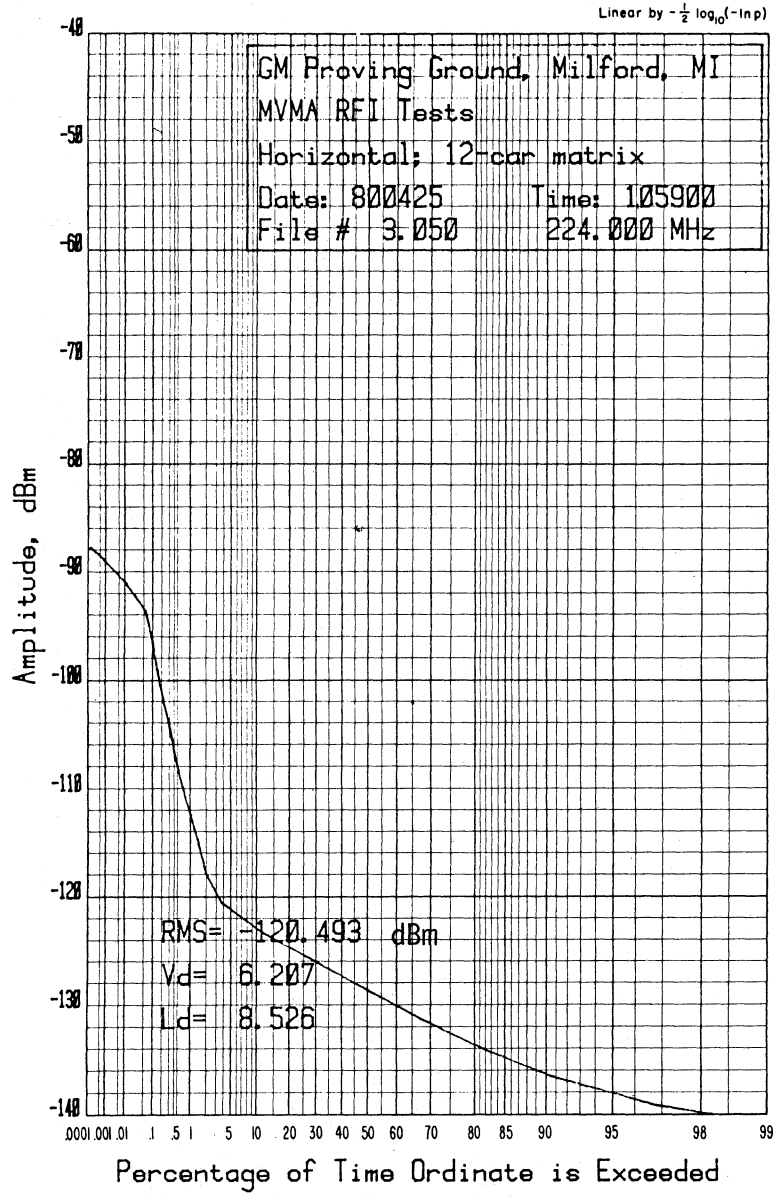

Figure 30. APD, 224 MHz - 12 Car Matrix

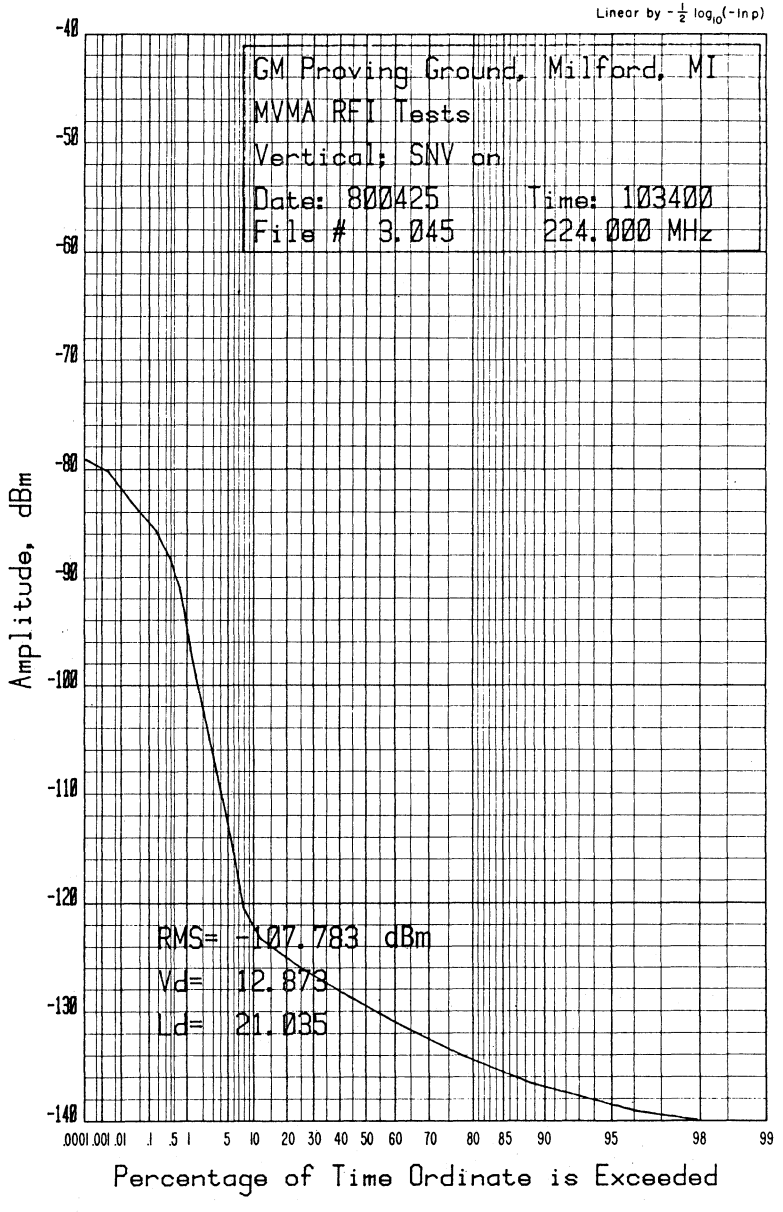

Figure 31. APD, 224 MHz - SNV

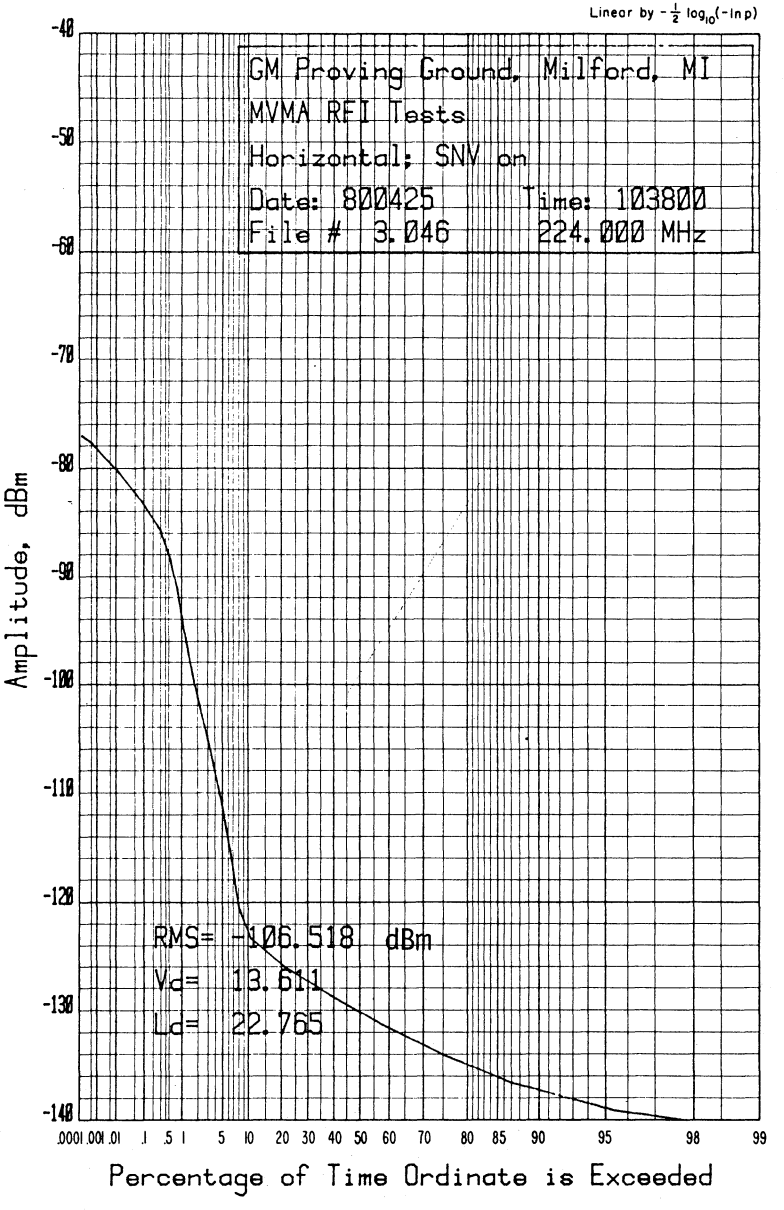

Figure 32. APD, 224 MHz - SNV

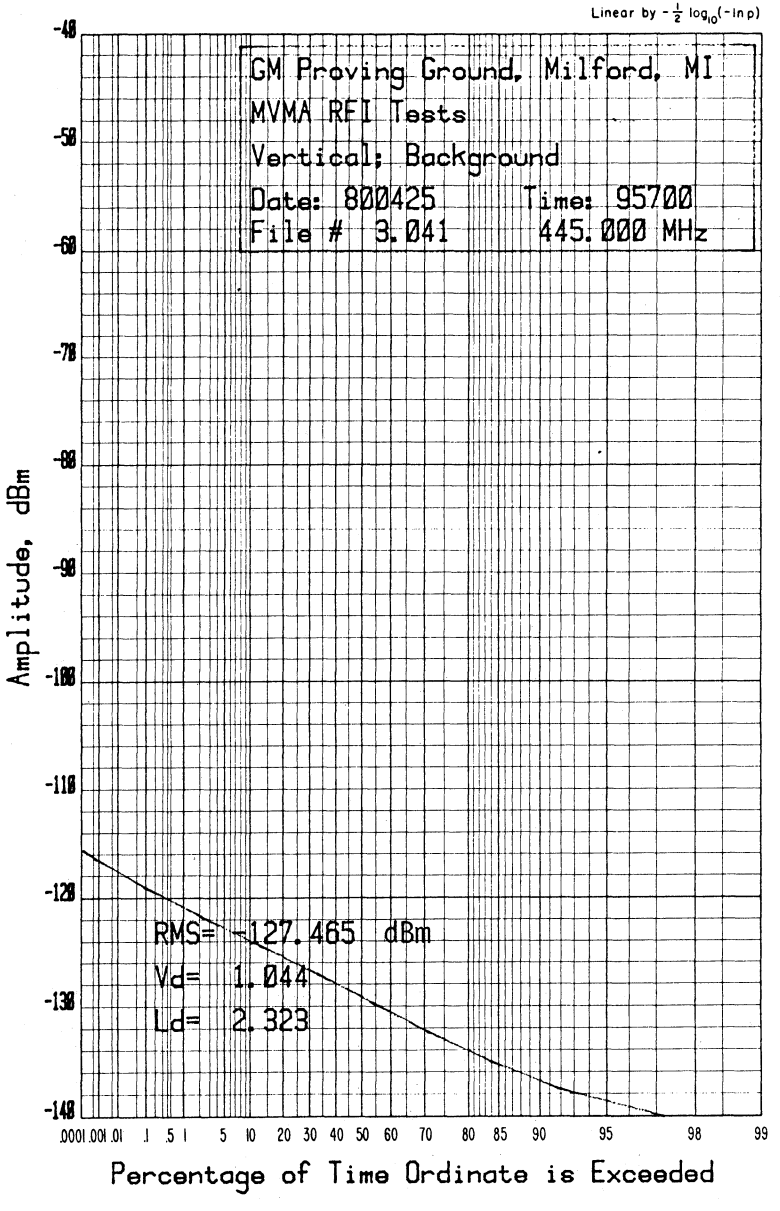

Figure 33. APD, 445 MHz - Background

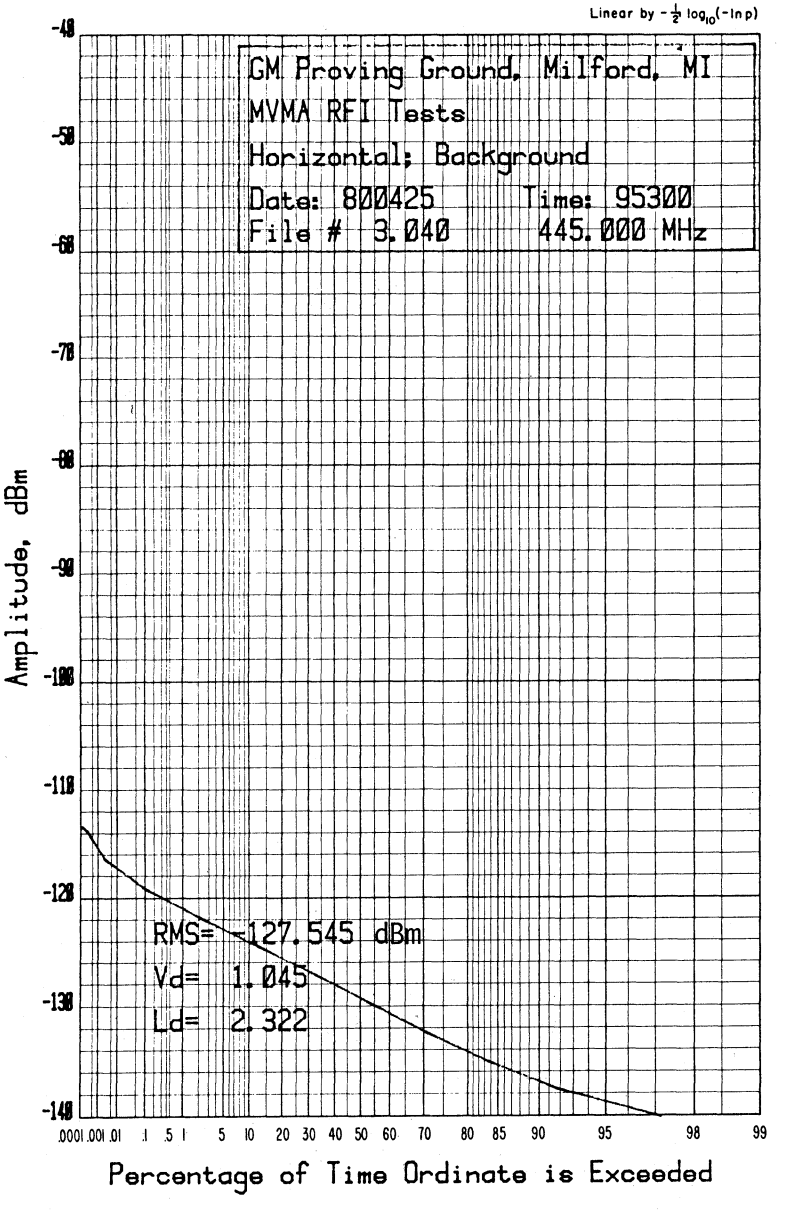

Figure 34. APD, 445 MHz - Background

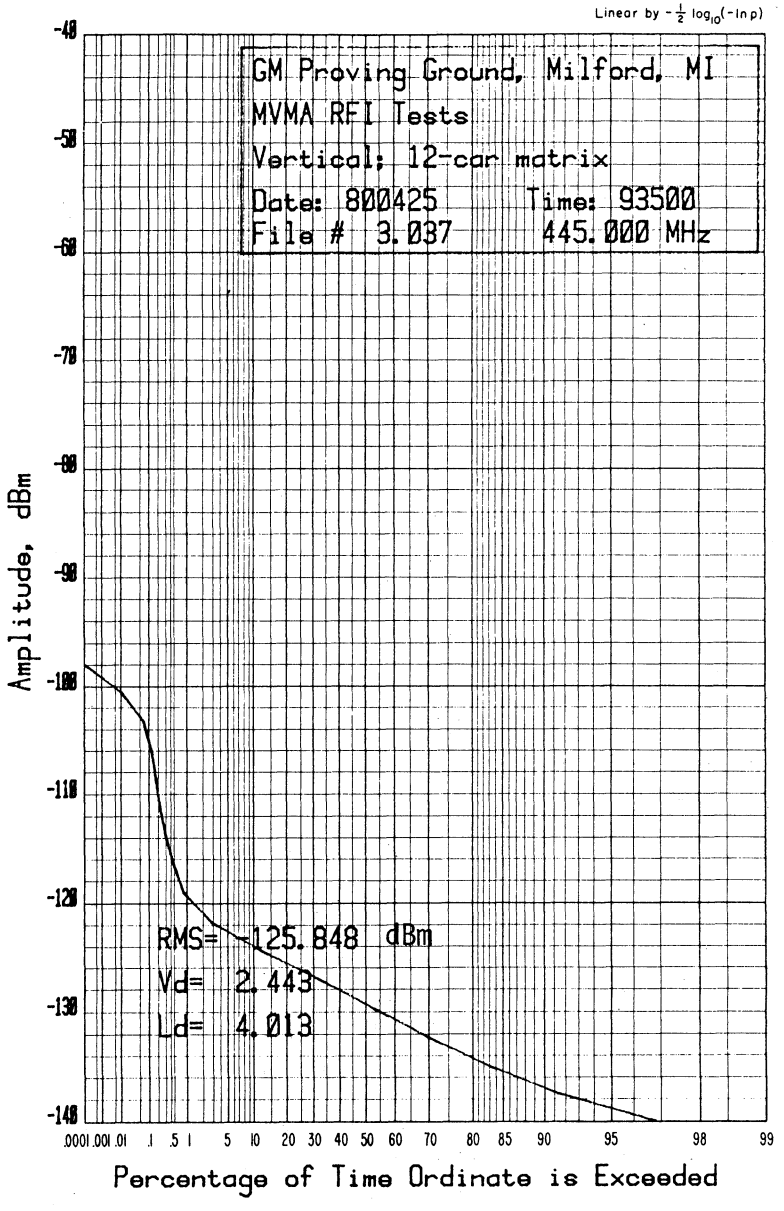

Figure 35. APD, 445 MHz, 12 Car Matrix

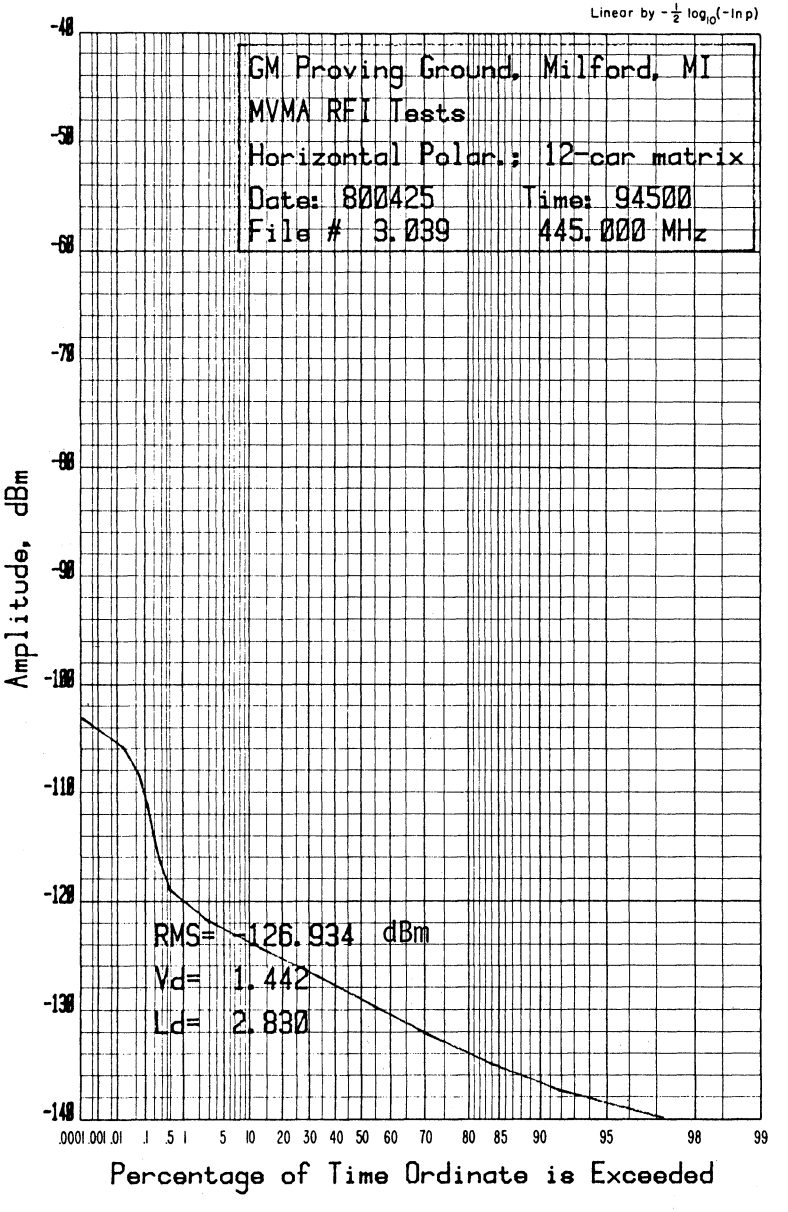

Figure 36. APD, 445 MHz, 12 Car Matrix

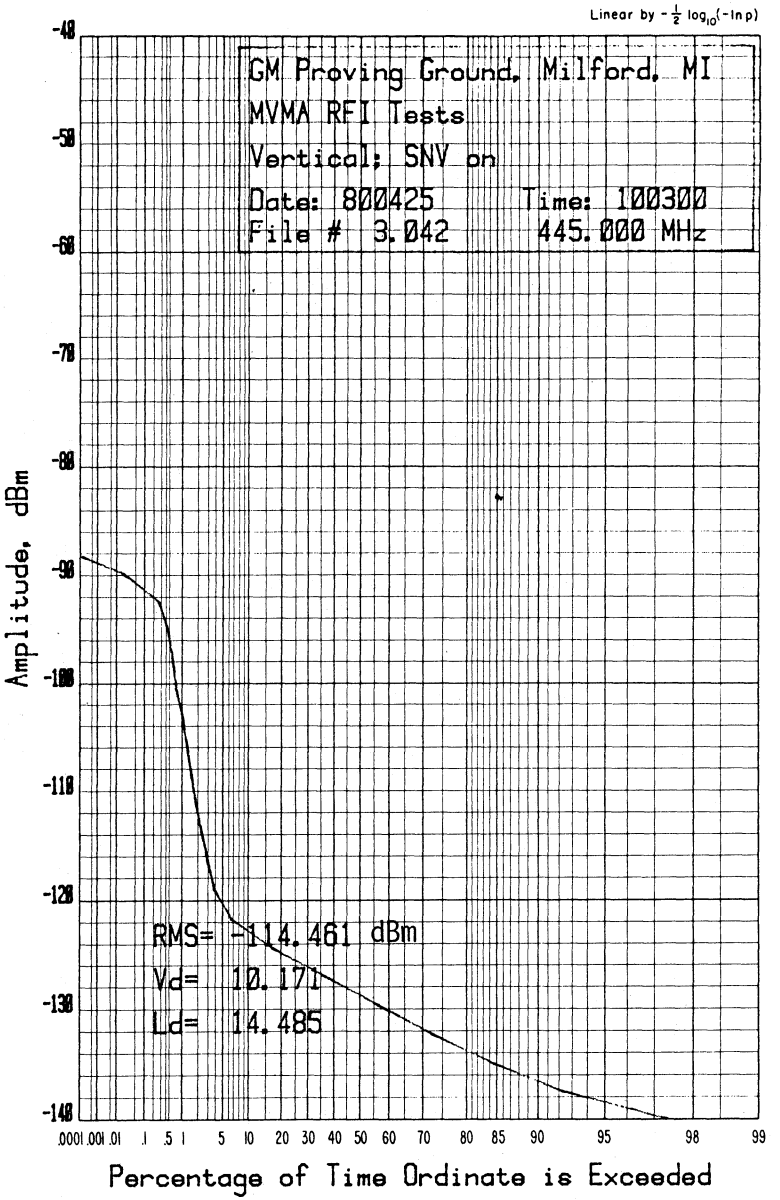

Figure 37. APD, 445 MHz - SNV

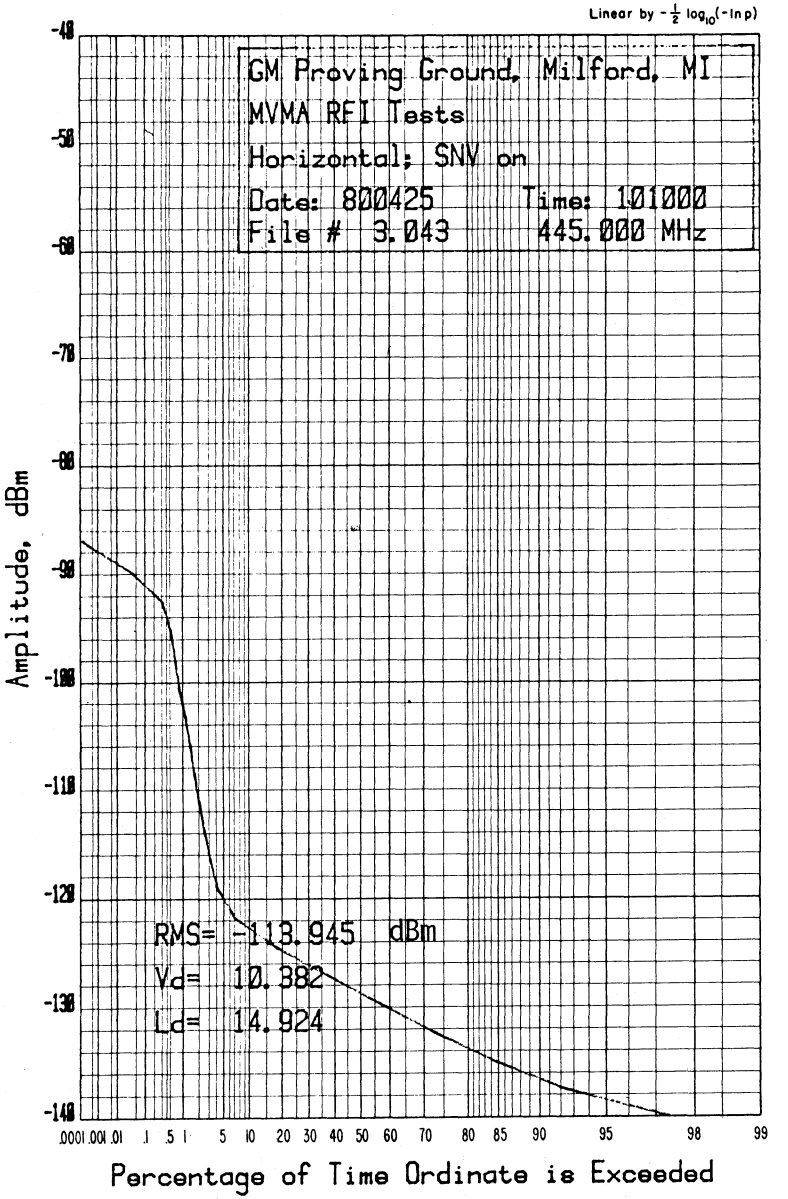

Figure 38. APD, 445 MHz - SNV

Table 2. Summary of Noise Measurements

Freq (MHz)	Fig.	Description	rms (dBm)	Antenna Factor K_1	dB> 1 μV/m	F_a Factor* K_2	F_a in** dB>KT
30.2 MHz	6	V, 12 CAR	-109	104.6	-4.4	29.4	25
30.2 MHz	7	H, 12 CAR	-110	105.6	-4.4	29.4	25
30.2 MHz	8	V, SNV	-102	104.6	+2.6	29.4	32
30.2 MHz	9	H, SNV	-99	105.6	+6.6	29.4	36
47 MHz	17	V, 12 CAR	-109	109.0	0	25.5	25.5
47 MHz	18	H, 12 CAR	-114	109.1	-4.9	25.5	20.6
47 MHz	19	V, SNV	-105	109.0	+4.0	25.5	29.5
47 MHz	20	H, SNV	-98	109.1	+11.1	25.5	36.6
147 MHz	23	V, 12 CAR	-118	120.5	+2.5	15.6	18.1
147 MHz	24	H, 12 CAR	-118	120.5	+2.5	15.6	18.1
147 MHz	25	V, SNV	-104	120.5	+16.5	15.6	32.1
147 MHz	26	H, SNV	-103	120.5	+17.5	15.6	33.1
224 MHz	29	V, 12 CAR	-123	125.0	+2.0	11.9	13.9
224 MHz	30	H, 12 CAR	-120	125.0	+5.0	11.9	16.9
224 MHz	31	V, SNV	-108	125.0	+17.0	11.9	28.9
224 MHz	32	H, SNV	-107	125.0	+18.0	11.9	29.9
445 MHz	35	V, 12 CAR	-126	130.0	+4.0	5.9	9.9
445 MHz	36	H, 12 CAR	-127	130.0	+3.0	5.9	8.9
445 MHz	37	V, SNV	-114	130.0	+16.0	5.9	21.9
445 MHz	38	H, SNV	-114	130.0	+16.0	5.9	21.9

* $F_a = E_n - 20 \log f - 10 \log B + 98.9$

$K_2 = -20 \log f_{MHz} - 10 \log B + 98.9$

** This data is graphed in Fig. 39

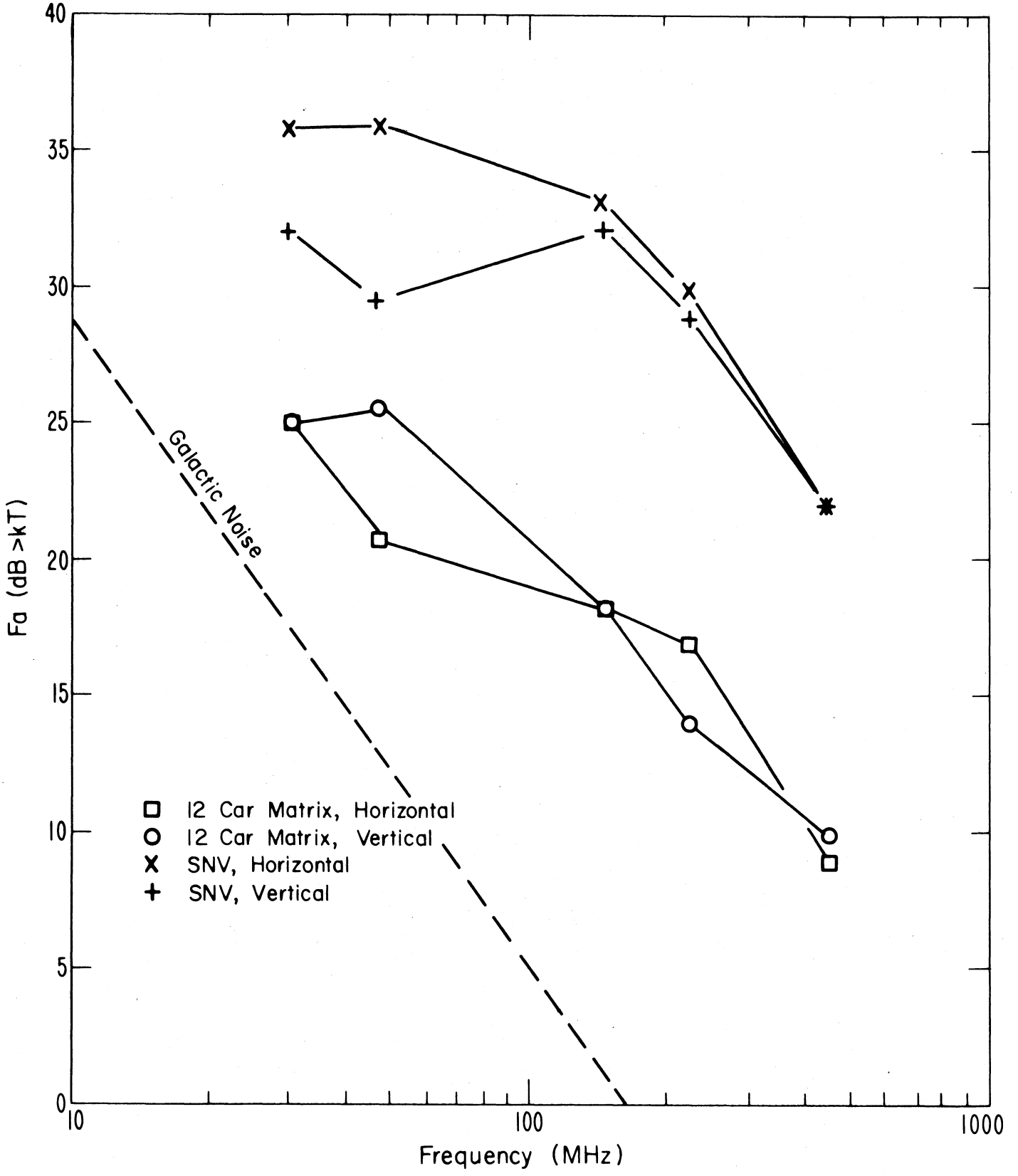

Fig. 39. Summary of Noise Measurements

6. REFERENCES

1. Hartman, W. J. (1980), Measurement of the effect of vehicle noise on land-mobile voice channels, NTIA Report 80-43.

2. Lauber, W. R., and J. M. Bertrand (1977), Preliminary urban VHF/UHF radio noise intensity measurements in Ottawa, Canada, Electromagnetic Compatibility 1977, Proceedings of 2nd Symposium on EMC, Montreux, Switzerland, June 28-30, pp. 357-362, IEEE Catalog No. 77CH 1224-5EMC, 1977.

3. Spaulding, A. D. (1976), Man-made noise: the problem and recommended steps toward solution, OT Report 76-85.

FORM **NTIA-29**
(4-80)

U.S. DEPARTMENT OF COMMERCE
NAT'L. TELECOMMUNICATIONS AND INFORMATION ADMINISTRATION

BIBLIOGRAPHIC DATA SHEET

	1. PUBLICATION NO.	2. Gov't Accession No.	3. Recipient's Accession No.
	NTIA Report 80-54		

4. TITLE AND SUBTITLE
Measurements of Electromagnetic Noise Radiated From Automotive Ignition Systems

5. Publication Date
November 1980

6. Performing Organization Code
DOC/NTIA/ITS1

7. AUTHOR(S)
Robert J. Matheson

9. Project/Task/Work Unit No.
9107123

8. PERFORMING ORGANIZATION NAME AND ADDRESS
Department of Commerce, National Telecommunications and Information Administration, Institute for Telecommunication Sciences, 325 Broadway, Room 3420, Boulder, CO 80303

10. Contract/Grant No.

11. Sponsoring Organization Name and Address

12. Type of Report and Period Covered
Technical Report

13.

14. SUPPLEMENTARY NOTES

15. ABSTRACT *(A 200-word or less factual summary of most significant information. If document includes a significant bibliography or literature survey, mention it here.)*

Measurements of the amplitude probability distributions and the average crossing rates of the electromagnetic noise radiated by automotive ignition systems were made at 30 MHz, 47 MHz, 147 MHz, 224 MHz and 445 MHz. The ignition noise from a single car and a 12-car matrix were each measured in a 10 kHz bandwidth, using a field-intensity meter, a DM-4, a desktop calculator, and an X-Y plotter. The DM-4 is an instrument built by NTIA to measure amplitude probability distributions and average crossing rates. Numerical integration of the amplitude probability distributions was used to determine the rms, the average, and the average logarithm of the envelope of the measured noise.

16. Key Words *(Alphabetical order, separated by semicolons)*
Amplitude Probability Distributions; Automotive Ignition Noise; Electromagnetic Noise; Noise Measurement.

17. AVAILABILITY STATEMENT

☒ UNLIMITED.

☐ FOR OFFICIAL DISTRIBUTION.

18. Security Class. *(This report)*
Unclassified

20. Number of pages
33

19. Security Class. *(This page)*
Unclassified

21. Price:

☆ U.S. GOVERNMENT PRINTING OFFICE: 1980—778-024/160 Region No. 8